Διέλευση φορτισμένων σωματιδίων από την ύλη

Απώλεια Ενέργειας λόγω Ιονισμού

Τύπος Bethe-Bloch

$$-\frac{dE}{dx} = \frac{4\pi}{m_e c^2} \cdot \frac{nz^2}{\beta^2} \cdot \left(\frac{e^2}{4\pi\varepsilon_0}\right)^2 \cdot \left[\ln\left(\frac{2m_e c^2 \beta^2}{I \cdot (1-\beta^2)}\right) - \beta^2\right]$$

β=υ/c, z ο ατομικός αριθμός του υλικού, ενώ το I εξαρτάται απ΄την ενέργεια ιονισμού του ατόμου.

Απώλειες ενέργειας φορτισμένων

Ιονισμός

Ελάχιστος ιονισμός

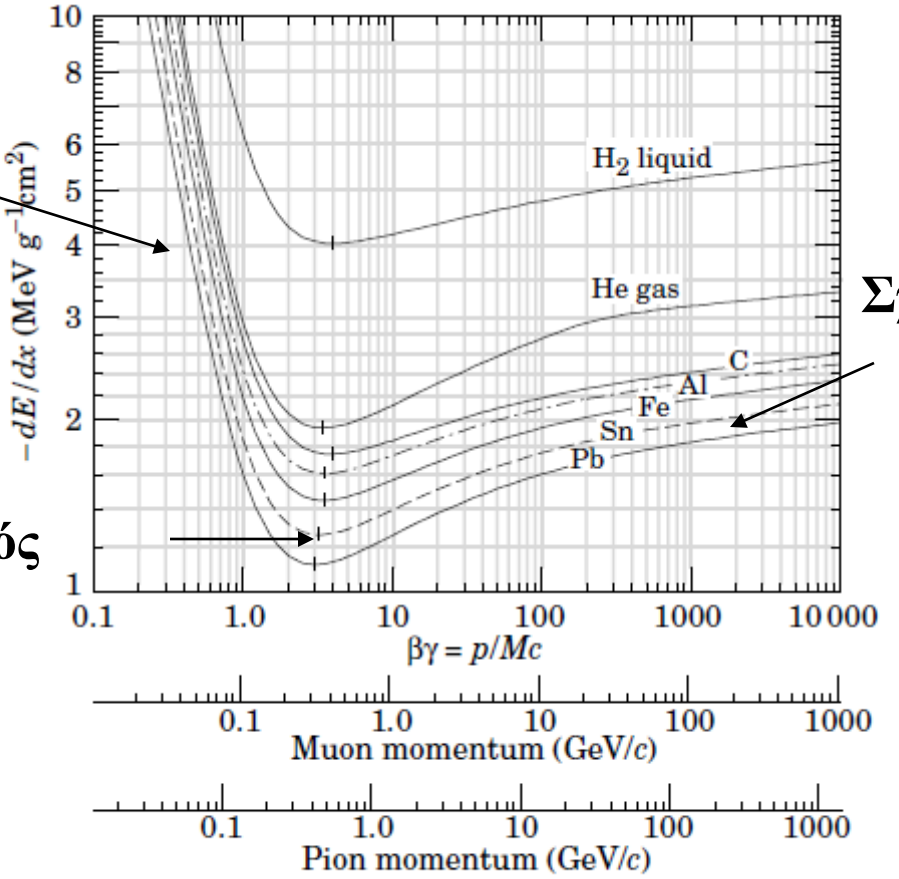

Σχετικιστική αύξηση

Στις χαμηλές ταχύτητες γ<2, ο ιονισμός εξαρτάται από τον χρόνο περάσματος του σωματιδίου από το άτομο. Στις σχετικιστικές ταχύτητες αυξάνονται οι συνιστώσες του ηλεκτρικού πεδίου οι κάθετες προς την κίνηση και αντίστοιχα ο όγκος που ιονίζεται.Στη συνέχεια λόγω πόλωσης σταθεροποιείται η απώλεια ενέργειας περίπου στα 2 MeV/g cm^2

Πειραματική μέτρηση dE/dX σε αναλογικό θάλαμο αερίου

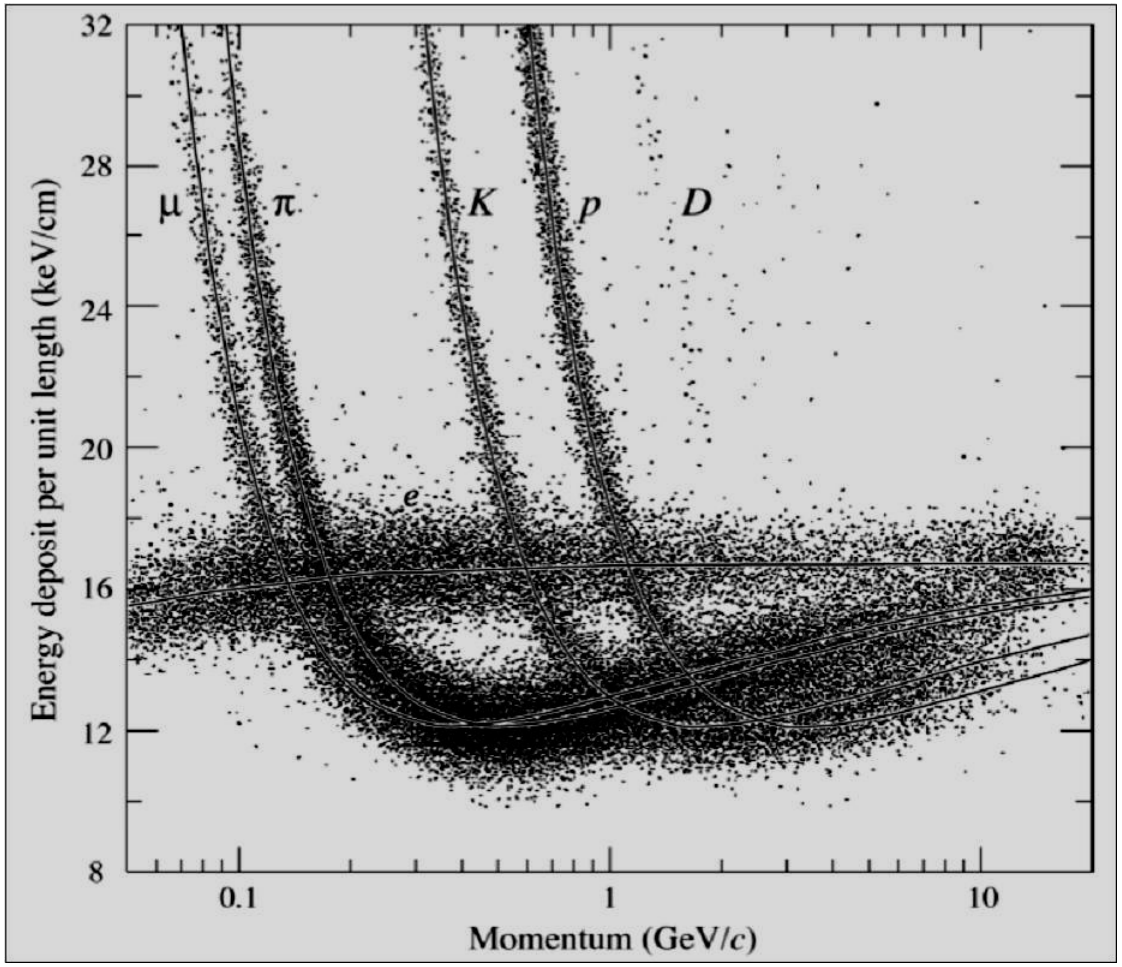

Πολλαπλή σκέδαση (multiple scattering)

$$\varphi_{\text{rms}} = \left(\frac{zE_s}{pv}\right)\sqrt{\frac{t}{X_0}} \qquad E_s = (4\pi/\alpha)^{1/2}\, mc^2 = 21\,\text{MeV}$$

Here r_e is the classical radius of the electron and $\alpha = 1/137$. Thus a singly charged particle with a value of $pv = p\beta c$ measured in MeV will suffer an rms deflection of $21/(pv)$ radians in traversing one radiation length.

Μήκος ακτινοβολίας X_0

$$\frac{1}{X_0} = 4\alpha\left(\frac{Z}{A}\right)(Z+1)\, r_e^2 N_0 \ln\left(\frac{183}{Z^{1/3}}\right)$$

Ακτινοβολία πέδησης (bremstralung)

Η ακτινοβολία πέδησης εκπέμπεται κατά την επιτάχυνση του ηλεκτρονίου από το ηλεκτρικό πεδίο του πυρήνα. Το φάσμα εκπομπής είναι συνεχές.

$$\frac{dE}{dx} = -\frac{N}{A}\int_0^{E-mc^2} \sigma_{br}(E,k)k\,dk \ ,$$

Το ολοκλήρωμα για όλα τα μήκη κύματος, δίνεται από :

$$\frac{dE}{dx} = \frac{4NZ}{A}\alpha r_e^2 E\left[\ln 191Z^{-1/3} + 1/18\right]$$

Χρησιμοποιώντας το μήκος ακτινοβολίας η σχέση απλοποιείται σε:

$$\left\langle \frac{\mathrm{d}E}{\mathrm{d}x} \right\rangle_{\mathrm{rad}} = -\frac{E}{X_0} \qquad \langle E \rangle = E_0 \exp\left(-\frac{x}{X_0}\right)$$

Μήκος ακτινοβολίας

$$X_0 \equiv \left[\frac{4NZ(Z+1)}{A}\alpha r_e^2 \ln\left(191Z^{-1/3}\right)\right]^{-1}$$

Σε προσέγγιση:

$$X_0 \simeq 10^3 \times \frac{A}{6Z(Z+1)}\ \mathrm{g.cm}^{-2}$$

Για ένωση ή μίγμα:

$$\frac{1}{X_0} = \sum_i \frac{w_i}{X_0^i},$$

$$X_0(\mathrm{air}) = 36.9\ \mathrm{g/cm}^2$$

Ακτινοβολία Πέδησης για μιόνια

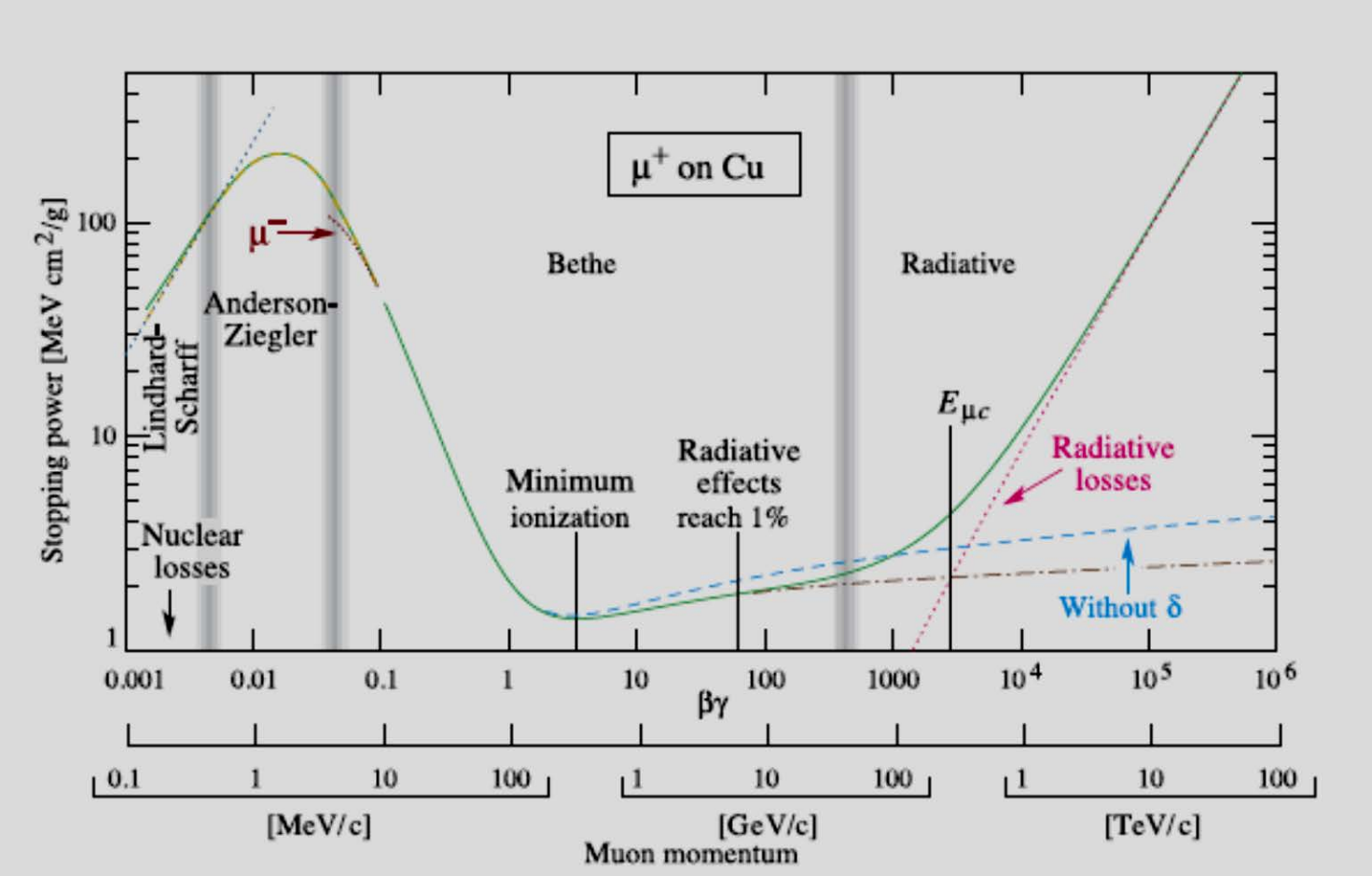

Δίδυμη Γένεση.

Μια ακτίνα γ με ενέργεια μεγαλύτερη από 2 μάζες ηλεκτρονίου,δημιουργεί ένα ζευγάρι e^+ e^- . Η διαδικασία γίνεται στο ηλεκτρικό πεδίο ενός πυρήνα για διατήρηση της ορμής.

Η διαδικασία συνδέεται με την ακτινοβολία πέδης αν μεταφέρουμε το ηλεκτρόνιο στο δεξί μέρος της αντίδρασης. (γίνεται ποζιτρόνιο και εξέρχεται από την κορυφή της αντίδρασης.)

Η μέση απόσταση που διανύει το φωτόνιο μέχρι τη δημιουργία, ονομάζεται μήκος μετατροπής. Το μήκος εξαρτάται από την ενέργεια αλλά για υψηλές ενέργειες γίνεται ίσο με 9/7 X_0.

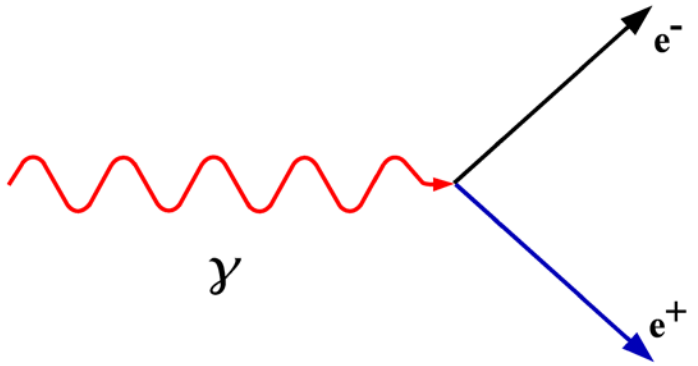

Ενεργός Διατομή για παραγωγή ζεύγους.

$$1 << \frac{\hbar\omega}{m_e c^2} << \frac{1}{Z^{\frac{1}{3}}}$$

$$\sigma_{pair} = ar^2 Z^2 \left[\frac{28}{y} ln\left(\frac{2\hbar\omega}{m_e c^2} \right) - \frac{218}{27} \right] (m^2 / atom)$$

with screening

$$\sigma_{pair} = ar^2 Z^2 \left[\frac{28}{y} ln\left(\frac{2\hbar\omega}{m_e c^2} \right) - \frac{2}{27} \right] (m^2 / atom)$$

Διατομή για δίδυμη γένεση

Διαφορική διατομή για δίδυμη γένεση. x=E/k. E η μεταφορά ορμής στο ζεύγος, k η ενέργεια του φωτονίου.

$$\frac{d\sigma}{dx} = \frac{A}{X_0 N_A}\left[1 - \tfrac{4}{3}x(1-x)\right]$$

Μετά την ολοκλήρωση, η ενεργός διατομή στο όριο υψηλής ενέργειας.

$$\sigma = \tfrac{7}{9}(A/X_0 N_A)$$

Ακτινοβολία Cerenkov

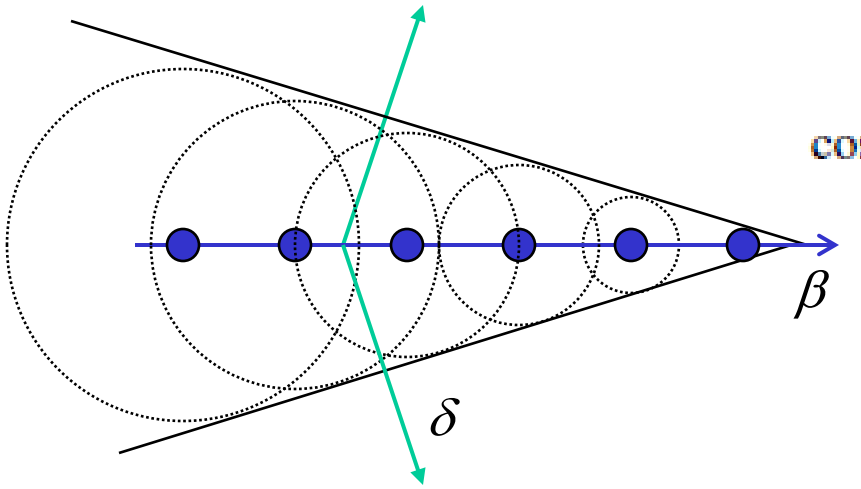

$$\cos\theta = \frac{(ct/n)}{\beta ct} = \frac{1}{\beta n}, \quad \beta > \frac{1}{n}$$

$$n = 1.0003$$

$$\beta = 1/n$$

$$E_{Thr} = \frac{mc^2}{\sqrt{1-\beta^2}}$$

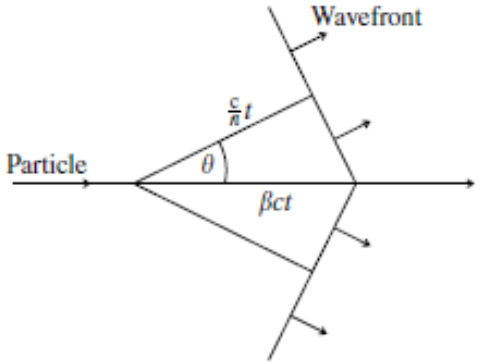

Υπολογισμός ενέργειας κατωφλίου

e^- mc^2 = 0,51 MeV E_T = 21 MeV

μ^- mc^2 = 106 MeV E_T = 4.3 GeV

Ακτινοβολία Cerenkov

$$\frac{\partial^2 N}{\partial x \partial \lambda} = 2\pi\alpha\left(1-\frac{1}{\beta^2 n^2}\right)\frac{1}{\lambda^2}$$

Ο αριθμός των φωτονίων που εκπέμπονται είναι αντιστρόφως ανάλογος του μήκους κύματος. Δηλαδή έχουμε περισσότερα στο υπεριώδες ιώδες και μπλε. Συνήθως το υπεριώδες απορροφάται από το υλικό και ανιχνεύουμε κυρίως το μπλε

$$\frac{\partial N}{\partial x} = 2\pi\alpha\left(1-\frac{1}{\beta^2 n^2}\right)\left(\frac{1}{\lambda_L}-\frac{1}{\lambda_H}\right)$$

Διαχωρισμός μιονίου από ηλεκτρόνιο

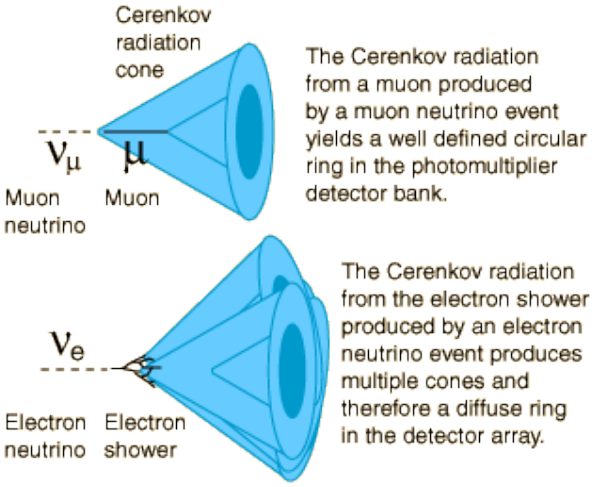

Ατμοσφαιρική φωταύγεια

Ένα μέρος της ενέργειας που χάνεται λόγω ιονισμού, μετατρέπεται σε φωτόνια του ορατού φάσματος. Προέρχονται από την αποδιέγερση των ατόμων του αζώτου και τα μήκη κύματος εκπέμπονται στην περιοχή 300-450 nm. Η εκπομπή των φωτονίων είναι ισότροπη προς όλες τις κατευθύνσεις. Εκπέμπονται περίπου 4,5 φωτόνια ανά μέτρο. Ο απιθμός των τροχιών σε ένα καταιονισμό υψηλής ενέργειας είναι μεγαλύτερος από 10^6 είναι δυνατή η ανίχνευση των καταιονισμών.

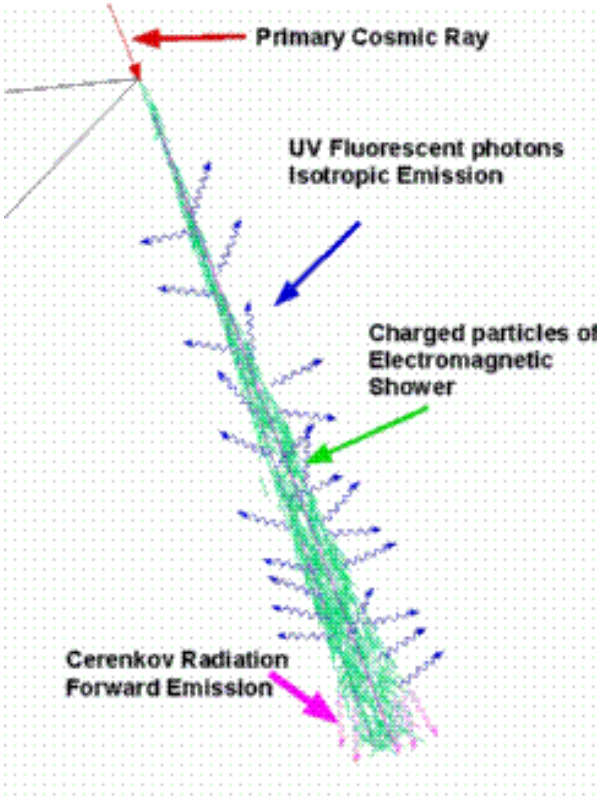

Αντίστροφη Σκέδαση Compton

Είναι γνωστό το φαινόμενο Compton κατά το οποίο ένα φωτόνιο σκεδάζεται σε ένα ατομικό ηλεκτρόνιο, μεταφέροντας ένα μέρος της ενέργειας του στο ηλεκτρόνιο.

Εάν το ηλεκτρόνιο έχει μεγάλη κινητική ενέργεια συμβαίνει τον αντίστροφο φαινόμενο δηλαδή το φωτόνιο να κερδίσει ενέργεια.

Για μία μετωπική κρούση, υπολογίζεται :

$$\hbar\omega = \frac{4}{3}\gamma^2 \hbar\omega_0$$

Αν ηλεκτρόνιο με γ=1000 (510 MeV)

σκεδαστεί με φωτόνιο R.F. $\nu = 10^9$ Hz $\rightarrow 10^{15}$ Hz (UV)

I.F $\nu = 3\times10^{12}$ Hz $\rightarrow 3\times10^{18}$ (x-ray)

visual $\nu = 4\times10^{14}$ Hz $\rightarrow 4\times10^{20}$ (γ 1,6 MeV)

Σκέδαση Compton
Σχετικιστική

Σκέδαση Compton
Σχετικιστική

Ηλεκτρόνιο $\boldsymbol{P}=\left[\gamma m_e\vec{v},\gamma m_e\right]$ $\boldsymbol{P'}=\left[\gamma' m_e\vec{v}',\gamma' m_e\right]$

Φωτόνιο $\boldsymbol{K}=\left[\frac{\hbar\omega}{c}\hat{k},\frac{\hbar\omega}{c^2}\right]$ $\boldsymbol{K'}=\left[\frac{\hbar\omega'}{c}\hat{k}',\frac{\hbar\omega'}{c^2}\right]$

Διατήρηση $4-Ορμής$

$P+K=P'+K'\rightarrow\left(P+K\right)^2=\left(P'+K'\right)^2$

$\boldsymbol{P}^2+2\boldsymbol{PK}+\boldsymbol{K}^2=\boldsymbol{P'}^2+2\boldsymbol{PK}+\boldsymbol{K'}^2$

$\boldsymbol{P}^2=\boldsymbol{P'}^2=\boldsymbol{m}_e^2\boldsymbol{c}^4 \qquad \rightarrow \boldsymbol{K}^2=\boldsymbol{K'}^2=0$

$\rightarrow \boldsymbol{PK}=\boldsymbol{P'K'}$

$\boldsymbol{(P+K)K'}=\boldsymbol{(P'+K')K'} \quad \boldsymbol{PK'}+\boldsymbol{KK'}=\boldsymbol{P'K'}+\boldsymbol{K'K'}$

(i) $\boldsymbol{PK'}+\boldsymbol{KK'}=\boldsymbol{P'K'}$ ←

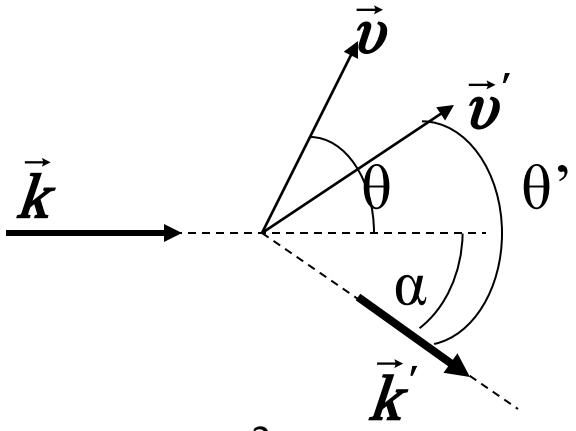

$$\cos a = \vec{i}_k \cdot \vec{i}_{k'}$$

$$\cos\theta = \vec{i}_k \cdot \vec{v}$$

$$\cos\theta' = \vec{i} \cdot \vec{v}$$

$$KK' = \left(\frac{\hbar}{c}\right)^2 \omega\omega' \cos a - \left(\frac{\hbar}{c^2}\right)^2 \omega\omega'$$

$$PK' = \gamma m_e \frac{\hbar}{c} \omega' v \cos\theta' - \gamma m_e \frac{\hbar}{c^2} \omega'$$

$$PK = \gamma m_e \frac{\hbar}{c} \omega v \cos\theta - \gamma m_e \frac{\hbar}{c^2} \omega$$

Αντικαθιστώντας στην (i) υπολογίζουμε:

$$\frac{\omega'}{\omega} = \frac{\frac{v}{c}\cos\theta - 1}{\left(\frac{v}{c}\cos\theta - 1\right) + \frac{\hbar\omega}{\gamma m_e c^2}\left(\cos a - 1\right)}$$

Σε πρώτη προσέγγιση αν υ=0, γ=1

$$\frac{\omega'}{\omega} = \frac{1}{1 + \frac{\hbar\omega}{\gamma m_e c^2}(1 - \cos a)}$$

$$\frac{\Delta\lambda}{\lambda} = \frac{\lambda' - \lambda}{\lambda} = \frac{\hbar\omega}{m_e c^2}(1 - \cos a)$$

$$\frac{\omega'}{\omega} = \frac{1 - \frac{\upsilon}{c}\cos\theta}{1 - \frac{\upsilon}{c}\cos\theta'}$$

$$\hbar\omega << \gamma m_e c^2$$

$$\frac{\Delta\omega}{\omega} = \frac{\cos\theta - \cos\theta'}{1 - \frac{\upsilon}{c}\cos\theta'}$$

Αντίστροφη Σκέδαση Compton

Είναι γνωστό το φαινόμενο Compton κατά το οποίο ένα φωτόνιο σκεδάζεται σε ένα ατομικό ηλεκτρόνιο, μεταφέροντας ένα μέρος της ενέργειας του στο ηλεκτρόνιο.

Εάν το ηλεκτρόνιο έχει μεγάλη κινητική ενέργεια συμβαίνει τον αντίστροφο φαινόμενο δηλαδή το φωτόνιο να κερδίσει ενέργεια.

Για μία μετωπική κρούση, υπολογίζεται :

$$\hbar\omega = \frac{4}{3}\gamma^2 \hbar\omega_0$$

Αν ηλεκτρόνιο με γ=1000 (510 MeV)

σκεδαστεί με φωτόνιο R.F. $\nu = 10^9$ Hz $\rightarrow 10^{15}$ Hz (UV)

I.F $\nu = 3\times10^{12}$ Hz $\rightarrow 3\times10^{18}$ (x-ray)

visual $\nu = 4\times10^{14}$ Hz $\rightarrow 4\times10^{20}$ (γ 1,6 MeV)

Φορτισμένο σωματίδιο κινείται στην ύλη με σχετικιστική ταχύτητα.

Η απόδειξη των μετασχηματισμών του Η.Μ. πεδίου είναι αρκετά προχωρημένη και αντιστοιχεί στην ύλη του Η.Μ. ΙΙ.
Θα δώσουμε μια «γεωμετρική» ερμηνεία που γίνεται εύκολα κατανοητή.

Στην κλασική περιγραφή του Ηλεκτρικού πεδίου χρησιμοποιούμε για την αναπαράσταση, τις δυναμικές γραμμές.

Η ένταση του πεδίου αντιστοιχεί στην πυκνότητα των δυναμικών γραμμών.

Παρατηρητής που κινείται μαζί με το φορτίο

- Ο αδρανειακός παρατηρητής που κινείται μαζί με το φορτίο, «βλέπει» τις δυναμικές γραμμές να είναι ακτινικές και με σταθερή πυκνότητα σε κάθε κατεύθυνση.
- Αν θεωρήσει μια επιφάνεια dS΄ η πυκνότητα των δυναμικών γραμμών θα είναι n=dN/dS’.
- Προφανώς αν η επιφάνεια $dS_x΄$ είναι κάθετη στον άξονα x , $dS_x=dS_x΄$
- Όταν η dS_y’ είναι κάθετη στον άξονα y, $dS_y=dS_y΄/\gamma$

Ακίνητος παρατηρητής

Ο ακίνητος παρατηρητής βλέπει την επιφάνεια $\mathbf{dS_x = dS_x'}$ γιατί οι πλευρές της είναι κάθετες στην κίνηση, ενώ την $\mathbf{dS_y = dS_y'/\gamma}$.

Ο αριθμός των δυναμικών γραμμών είναι ο ίδιος και στα δύο συστήματα.

Άρα η ένταση $\mathbf{E_x'}$ θα είναι ίση με την $\mathbf{E_x}$, ενώ η $\mathbf{E_y = \gamma E_y}$.

$$E_x = E'_x$$

$$E_y = \gamma E'_y$$

Γεωμετρία

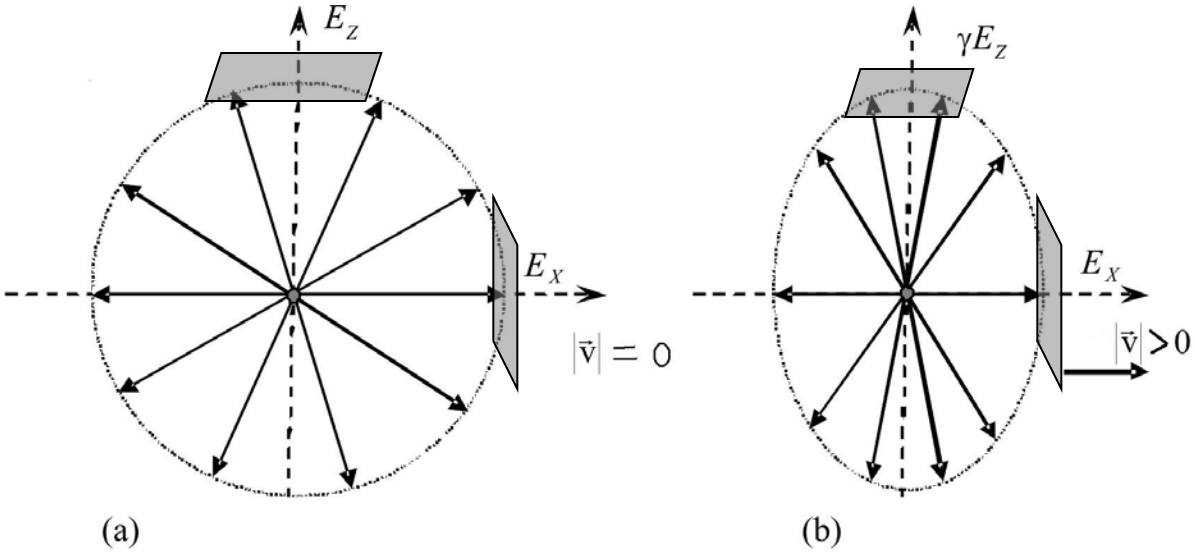

Αν τα βέλη αντιστοιχούν στις δυναμικές γραμμές, η πυκνότητα τους αυξάνει γύρω από τον άξονα y και ελαττώνεται γύρω από τον άξονα x.

Ο προηγούμενος συλλογισμός, δεν είναι απόδειξη για τον μετασχηματισμό των Η.Μ. πεδίων, αλλά περιγραφή του Ηλ. πεδίου, όπως το βλέπει ο παρατηρητής στο σύστημα εργαστηρίου.

Το παραπάνω ισχύει όταν στο κινούμενο σύστημα, το μαγνητικό πεδίο είναι μηδέν.

Το πεδίο που βλέπει το ακίνητο ηλεκτρόνιο

Στον υπολογισμό του ιονισμού και της σκέδασης, το ακίνητο ατομικό ηλεκτρόνιο, βλέπει το φορτισμένο σωματίδιο να κινείται με ταχύτητα υ πάνω στο άξονα x σε απόσταση r .

Το ηλεκτρικό πεδίο $\vec{E}$ έχει συνιστώσες :

$$E_{\perp} = \frac{q}{4\pi\varepsilon_0 \sqrt{1 - v^2/c^2}} \frac{1}{\sqrt{y^2 + z^2}} = \gamma E'_{\perp}(t)$$

$$E_x = \frac{q(1 - v^2/c^2)}{4\pi\varepsilon_0 (x - vt)^2}$$

Η απόσταση x στο σύστημα εργαστηρίου, αντιστοιχεί σε απόσταση x'=γx στο σύστημα του κινούμενου φορτίου.

Το ηλεκτρικό πεδίο για να φθάσει στη θέση x , χρειάζεται χρόνο t .

Σχετικιστικός Μετασχηματισμός Ηλεκτρικού και Μαγνητικού Πεδίου

$$E'_x = E_x \qquad B'_x = B_x$$

$$E'_y = \frac{E_y - \frac{v}{c} B_z}{\sqrt{1 - v^2/c^2}} \qquad B'_y = \frac{B_y + \frac{v}{c^2} E_z}{\sqrt{1 - v^2/c^2}}$$

$$E'_z = \frac{E_z + \frac{v}{c} B_y}{\sqrt{1 - v^2/c^2}} \qquad B'_z = \frac{B_z - \frac{v}{c^2} E_y}{\sqrt{1 - v^2/c^2}}$$

Κινούμενο φορτίο

Στο σύστημα του φορτίου, το μαγνητικό πεδίο είναι μηδέν.

Άρα στο σύστημα εργαστηρίου, η διαμήκης συνιστώσα του ηλεκτρικού πεδίου διατηρεί την τιμή της, ενώ η εγκάρσιες πολλαπλασιάζονται με γ

$$B_x = B_y = B_z = 0 \quad \Rightarrow$$

$$E'_x = E_x$$

$$E'_y = \frac{E_y}{\sqrt{1 - v^2/c^2}}$$

$$E'_z = \frac{E_z}{\sqrt{1 - v^2/c^2}}$$

Υπολογισμός με μετασχηματισμό Lorentz

έστω S το σύστημα εργαστηρίου και S′ το σύστημα του σωματιδίου.

Θεωρούμε ότι τη στιγμή t=t′=0 , x=x′=0.

Στο S′ το διάνυσμα θέσης του ακίνητου ηλεκτρονίου είναι r′=(-υt′,0,b).

Στο σύστημα S′, το ηλεκτρικό πεδίο είναι ακτινικά συμμετρικό.

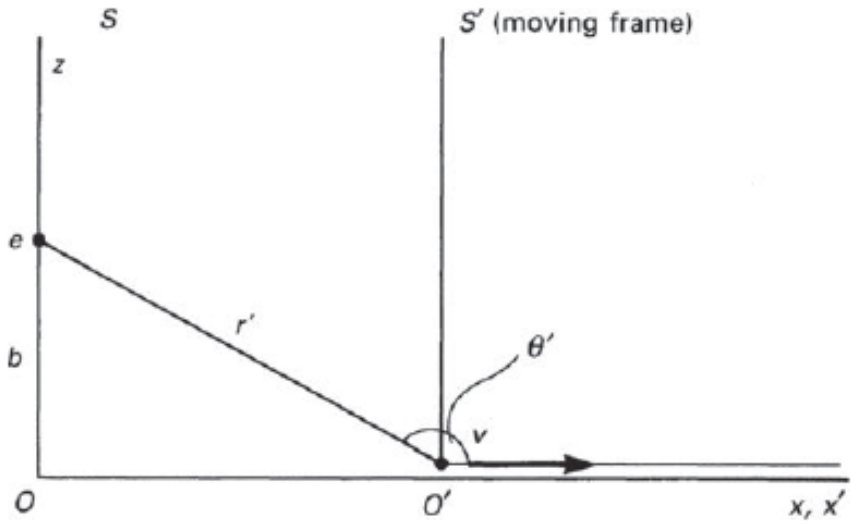

$$E'_x = \frac{ze}{4\pi\varepsilon_0}\frac{1}{r'^2}\cos\theta' = \frac{ze}{4\pi\varepsilon_0}\frac{x'}{r'^3}$$

$$E'_z = \frac{ze}{4\pi\varepsilon_0}\frac{1}{r'^2}\sin\theta' = \frac{ze}{4\pi\varepsilon_0}\frac{b}{r'^3}$$

$$r'^2 = vt'^2 + b^2$$

$$t' = \gamma(t - vx/t^2)$$

$$E'_x = -\frac{ze(\gamma vt)}{4\pi\varepsilon_0(b^2 + (\gamma vt)^2)^{\frac{3}{2}}}$$

$$E'_z = \frac{zeb}{4\pi\varepsilon_0(b^2 + (\gamma vt)^2)^{\frac{3}{2}}}$$

Χρησιμοποιώντας τον αντίστροφο μετασχηματισμό Lorentz:

$$E_x = E'_x$$
$$E_y = \gamma(E'_y - B'_z)$$
$$B'_x = B'_y = B'_z = 0$$

$$E_x = -\frac{ze(\gamma vt)}{4\pi\varepsilon_0 (b^2 + (\gamma vt)^2)^{\frac{3}{2}}}$$
$$E_z = \frac{ze\gamma b}{4\pi\varepsilon_0 (b^2 + (\gamma vt)^2)^{\frac{3}{2}}}$$
$$B_y = -\frac{ze\gamma vb}{4\pi\varepsilon_0 c^2 (b^2 + (\gamma vt)^2)^{\frac{3}{2}}}$$

Μορφή Ηλεκτρικού πεδίου

Το ηλεκτρικό πεδίο που δημιουργεί κινούμενο φορτίο. b είναι η παράμετρος κρούσης.

Από M. S. Longair

Η αύξηση της εγκάρσιας συνιστώσας του Ηλεκτρικού Πεδίου, αυξάνει τον ιονισμό στην σχετικιστικές ταχύτητες.

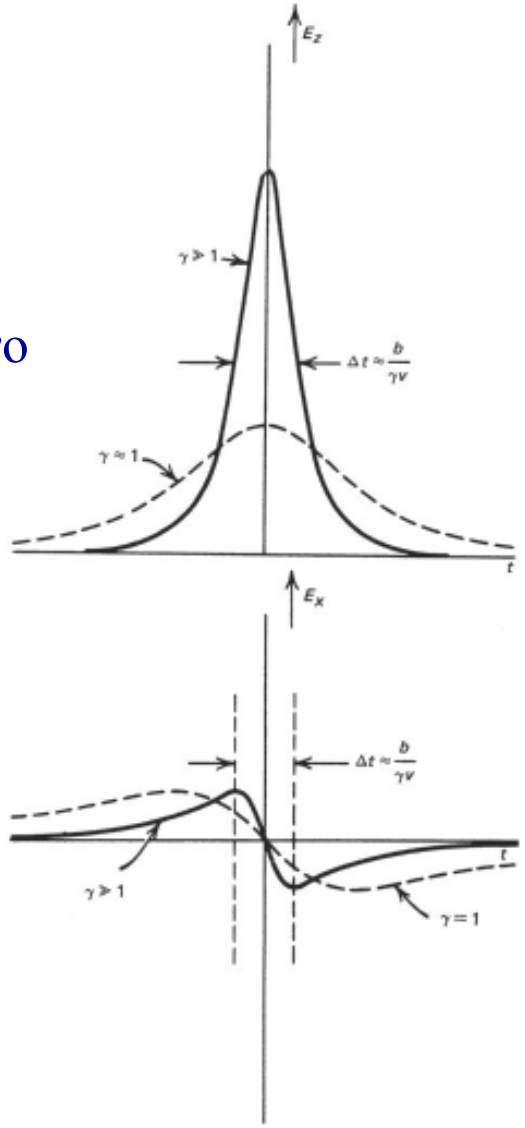

Αλλαγές όταν το σωματίδιο κινείται σχετικιστικά.

- Το ηλεκτρικό πεδίο $E_{\perp}$ που είναι κάθετο στην ταχύτητα, αυξάνεται κατά παράγοντα γ.
- Ο χρόνος «κρούσης» ελαττώνεται κατά παράγοντα 1/γ.
- Το ηλεκτρικό πεδίο E_x είναι μικρότερο από το E_z κατά παράγοντα 1/γ.
- Για πολύ μεγάλες ταχύτητες, $\upsilon \rightarrow c$, $E_z = cB_y$ και συμπεριφέρεται σαν Ημ. κύμα.

Υπολογισμοί στο σύστημα Κ.Μ.

Ενέργεια στο CM.

Δέσμη σωματιδίων μάζας m_1 και ενέργειας E, σε σωματίδιο στόχου μάζας m_2

$$P = (E, \vec{p})$$

$$P_o = (E_1 + E_2) - (\vec{p}_1 + \vec{p}_2)$$

$$\sqrt{s} = \sqrt{(E_1 + E_2)^2 - (\vec{p}_1 + \vec{p}_2)^2}$$

Το $\sqrt{s}$ είναι η ενέργεια που είναι διαθέσιμη στο CM.

Ελάχιστη ενέργεια για παραγωγή π^0 από δέσμη p

$$p + p \rightarrow p + p + \pi^0$$

$$\rightarrow \sqrt{s} \geq 2m_p + m_{\pi^0}$$

$$m_p = 0{,}938 \quad GeV,$$

$$m_{\pi^0} = 0{,}140 \quad GeV$$

$$\sqrt{s} \geq 2{,}01 \quad GeV$$

$$E_1 = (s - 2m_p)/2m_p$$

Ταχύτητα CM στο σύστημα εργαστηρίου

$$\beta_{CM} = \vec{p}_{1lab} / (E_{1lab} + m_2)$$

$$\gamma_{CM} = (E_{1lab} + m_2) / E_{CM}$$

Σε ένα πείραμα σταθερού στόχου, θεωρούμε ότι το σωμάτιο 2 είναι ακίνητο. Επίσης ότι η μάζα του είναι μικρή σε σχέση με την κινητική ενέργεια του σωματιδίου της δέσμης.

$$\vec{p}_2 = 0$$

$$\sqrt{s} = \sqrt{E_1^2 + E_2^2 - \vec{p}_1^2} = \sqrt{m_1^2 + m_2^2 + 2E_1 m_2}$$

$$p_1 >> m_1, m_1 \rightarrow \sqrt{s} = \sqrt{2E_1 m_2}$$

Διάσπαση στο σύστημα CM i

L

$\mathbf{Αρχ}\quad P$

$\mathbf{Τελ}\quad \boldsymbol{P_1, P_2}$

CM

$$\boldsymbol{P = (M,0,0,0)}$$

$$\boldsymbol{\vec{p}_1 = -\vec{p}_2}$$

$$\boldsymbol{E_1 + E_2 = \sqrt{m_1^2 + p^2} + \sqrt{m_2^2 + p^2} = M}$$

$$\boldsymbol{p = \frac{1}{2M}\sqrt{\left[M^2 - (m_1 - m_2)^2\right]\left[M^2 - (m_1 + m_2)^2\right]}}$$

$$\boldsymbol{M \geq m_1 + m_2}$$

Διάσπαση στο σύστημα CM ii

$$p_1^2 = p_2^2$$

$$E_1^2 - m_1^2 = E_2^2 - m_2^2$$

$$E_2^2 = E_1^2 - m_1^2 + m_2^2$$

$$(M - E_1)^2 = E_1^2 - m_1^2 + m_2^2$$

$$E_1 = \frac{1}{2M}(M^2 + m_1^2 - m_2^2)$$

$$E_2 = \frac{1}{2M}(M^2 + m_2^2 - m_1^2)$$

$$m_1 = m_2 = m$$

$$E_1 = E_2 = \frac{1}{2}M$$

$$p = \frac{1}{2}\sqrt{M2 - 4m^2}$$

Υπολογισμός στο Σύστημα Εργαστηρίου.

$$P = (E, 0, 0, p)$$

$$P_1 = (E_1, p_{1\perp}, p_{1z})$$

$$P_2 = (E_1, p_{2\perp}, p_{2z})$$

$$\vec{p}_\perp = \vec{p}_{1\perp} = -\vec{p}_{2\perp}$$

$$* \rightarrow CM$$

$$E_1 = \gamma(E_1^* + v p_{1z}^*)$$

$$p_{1z} = \gamma(p_{1z}^* + v E_1^*)$$

$$\gamma = \frac{E}{M} \qquad v = \frac{p}{E}$$

Παραγωγή μιονίων.

Όρια στην Ενέργεια Εργαστηρίου του παραγόμενου

$$\gamma(E_i^* - \beta p^*) \le E_i \le \gamma(E_i^* + \beta p^*)$$

$$\frac{dn}{d\Omega^*} = \frac{dn}{2\pi\, d(\cos\theta)} \prec \frac{dn}{dE_i} = constant$$

Η κανονικοποιημένη κατανομή ενέργειας των προιόντων γίνεται:

$$\frac{n_{ij}}{dE_i} = \frac{B_{ij}}{2\gamma\beta p^*} = \frac{B_{ij} M}{2 p^* P_L}$$

B_{ij} branching ratio j->i

---

p^* *CM momemtum*

P *Lab Momemtum*

$$\gamma\beta = \left(\frac{E}{M}\right)\left(\frac{P}{E}\right) = \frac{P}{M}$$

$$E_i = \gamma E_i^* + \gamma\beta p^* \cos\theta$$

$$dE_i = \gamma\beta p^* d(\cos\theta)$$

Παραγωγή μιονίων

Για την παραγωγή από $K^{\pm}$ έχουμε:

$$\frac{dn}{dE_\nu} = \frac{dn}{dE_\mu} = \frac{0,635}{(1 - m_\mu^2 / m_K^2)P_K}$$

Αποδεικνύεται ότι

$$\frac{< E_\mu >}{E_\pi} = 0.79$$

$$\frac{< E_n >}{E_\pi} = 0.21$$

Ο αριθμός των τελικών καταστάσεων είναι σταθερός αν εκφραστεί σαν συνάρτηση του κλάσματος της ενέργειας που παίρνει το τελικό σωματίδιο.

Τα όρια γίνονται :

$E_\mu(\mu^2/\mu_\pi^2) \leq E_\mu \leq E$

$0 \leq EE_\nu \leq (1-\mu^2/\mu_\pi^2)E$

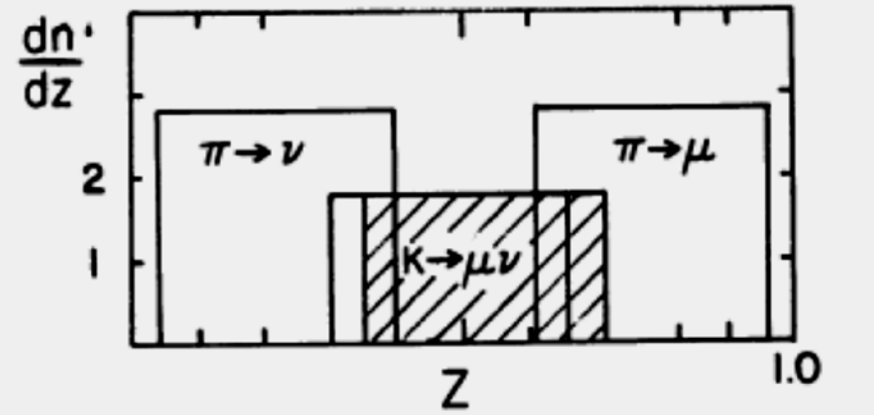

Figure 4.1: Decay distributions of π-decay and K-decay into $\mu\nu_\mu$ for 200 MeV/c parent mesons. z is the ratio of the total laboratory energy of the decay product to that of the parent.

$$\frac{< E_\mu >}{E_\pi} = 0.79$$

$$\frac{< E_\nu >}{E_\pi} = 0.21$$

Διάσπαση πιονίου, γωνία νετρίνου – μιονίου

$$E_1 + E_2 = \sqrt{m_1^2 + p_1^2} + \sqrt{m_2^2 + p_2^2}$$

$$\vec{p} = \vec{p}_1 + \vec{p}_2$$

$$(\vec{p}_2)^2 = (\vec{p} - \vec{p}_1)^2 \rightarrow$$

$$p_2^2 = p^2 + p_1^2 - 2\,p\;p_1 \cos\theta$$

$$p_1 = \frac{(M^2 + m_1^2 - m_2^2)p\cos\theta \pm 2E\sqrt{M^2 p^{*2} - m_1^2 p^2 \sin^2\theta_1}}{2(M^2 + p^2 \sin^2\theta_1)}$$

$$\frac{Mp^*}{m_1 p} > 1 \rightarrow \theta_1 > \frac{\pi}{2}$$

Φωτοπαραγωγή

$$\gamma + p \rightarrow p + \pi^0$$

$$s = (P_a + P_b)^2 = (P_c + P_d)^2$$

$$s = P_a^2 + P_b^2 + 2P_aP_b = P_a^2 + P_b^2 + (E_aE_b - p_ap_b)$$

$$= m_a^2 + m_b^2 + 2E_aE_b(1 - \beta_a\beta_b \cos\theta)$$

$$\beta = \frac{p}{E}$$

Αν p πρωτονίου =0

$$s = m_p^2 + 2E_\gamma p \geq (m_p + m_\pi)^2 = m_p^2 + 2m_pm_\pi + m_\pi^2$$

$$E_\gamma \geq m_\pi + \frac{m_\pi^2}{2m_p} \cong 145\ MeV$$

Παραγωγή $\bar{p}$

$$p + p \rightarrow pp\bar{p}p$$

$$s = 2m_p^2 + E_pm_p \geq 16m_p^2$$

$$E_p \geq 7m_p$$

Μεταφορά ορμής

$$t = (P_a - P_c)^2 = (P_b - P_d)^2$$

$$e^- + p \rightarrow e^- + p$$

$$t = (P_e - P_e')^2 = 2m_e^2 - 2E_e E_e' (1 - \beta_e \beta_e' \cos\theta)$$

$$Av\ \beta_e\ \beta_e' \rightarrow 1$$

$$m_e << E$$

$$\rightarrow$$

$$t = -2E_e E'_e\,(1 - \cos\theta) = -42E_e E'_e\ \sin^2 \theta/2$$

$$t = Q^2 = (P_e - P_e')^2 < 0 \rightarrow Virtual\ photon$$

$$\frac{d\sigma}{d\Omega} \prec \frac{1}{t^2} \prec \frac{1}{\sin^2 \theta/2}$$

Παραγωγή Ζεύγους

$$\gamma \rightarrow e^{+} + e^{-}$$

$$E_{\gamma} > 2m_e c^2$$

Κινητική $\mathbf{K = (\gamma\text{-}1) m_e c^2}$

Διατήρηση $4 - \boldsymbol{ορμής}$

$$\hbar\omega = 2\gamma m_e c^2$$

$$p_{\zeta} = 2\gamma m_e v = \frac{\hbar\omega}{c} \cdot \frac{v}{c}$$

Επειδή υ<c δεν αρκούν 2 σωματίδια για την διατήρηση της ορμής.

Αδρόνια

Διατομές σαν συνάρτηση της ενέργειας Κ.Μ.

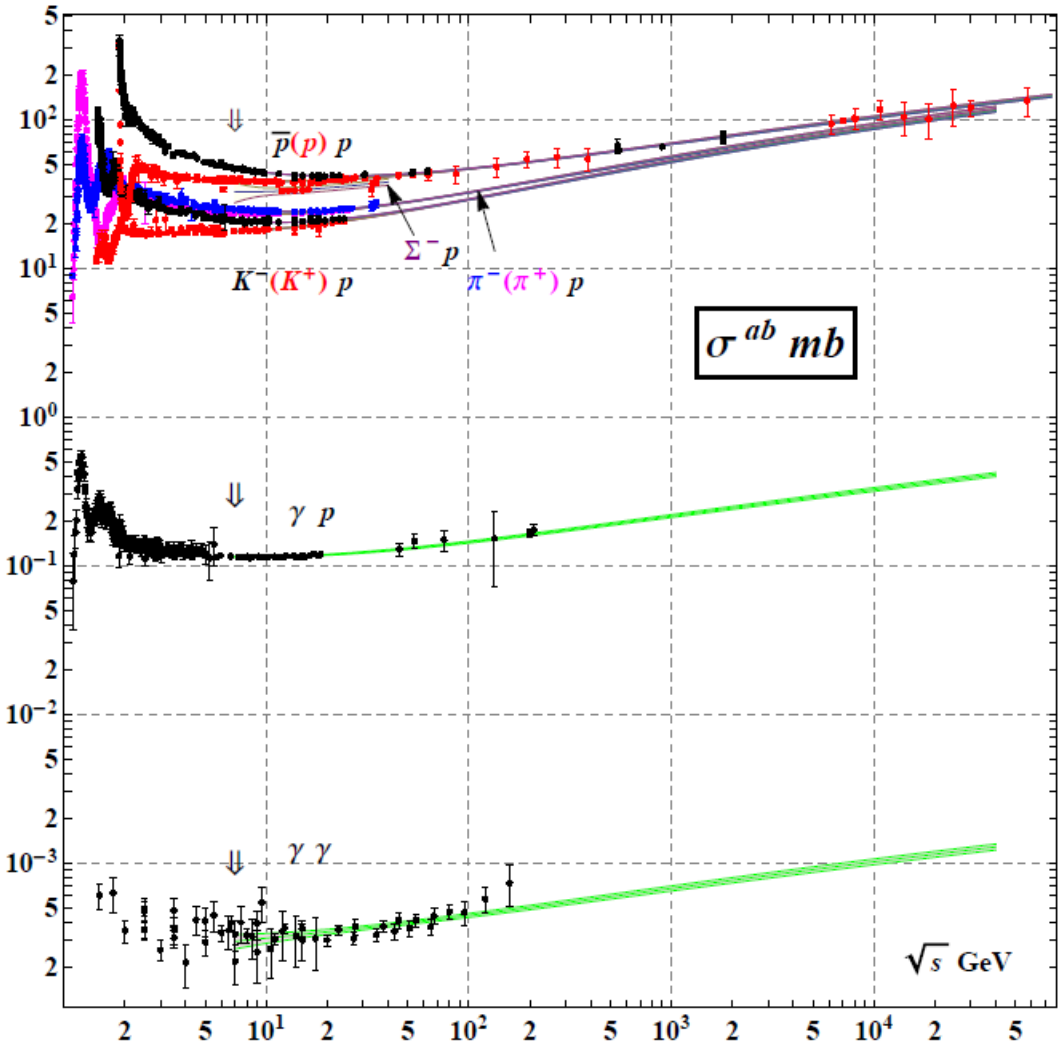

$log^2(s/s_0)$

Διατομή πρωτονίων αντιπρωτονίων

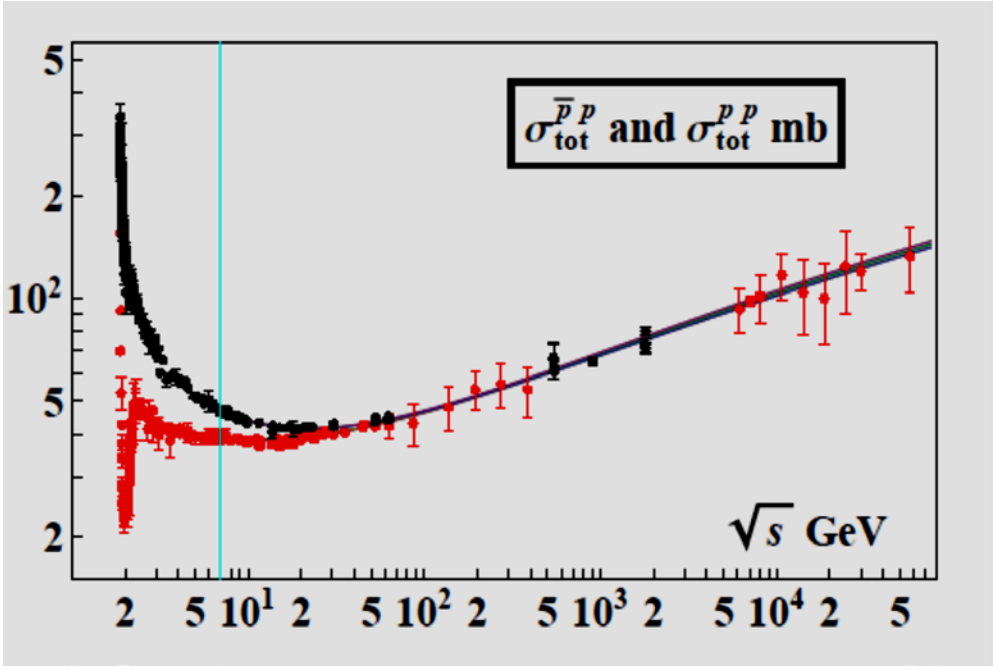

Διατομή π^+ π^-

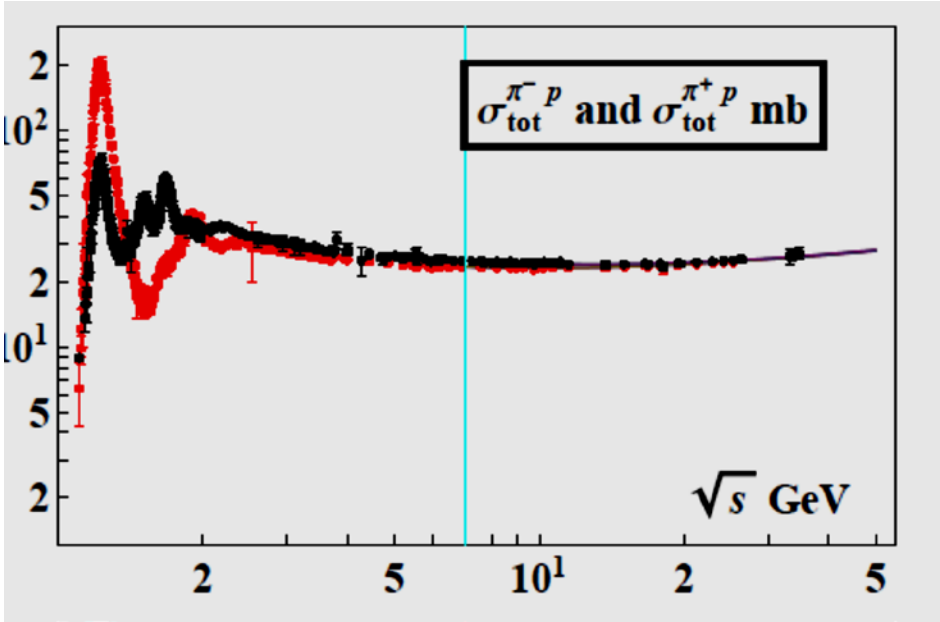

Διατομή φωτονίων

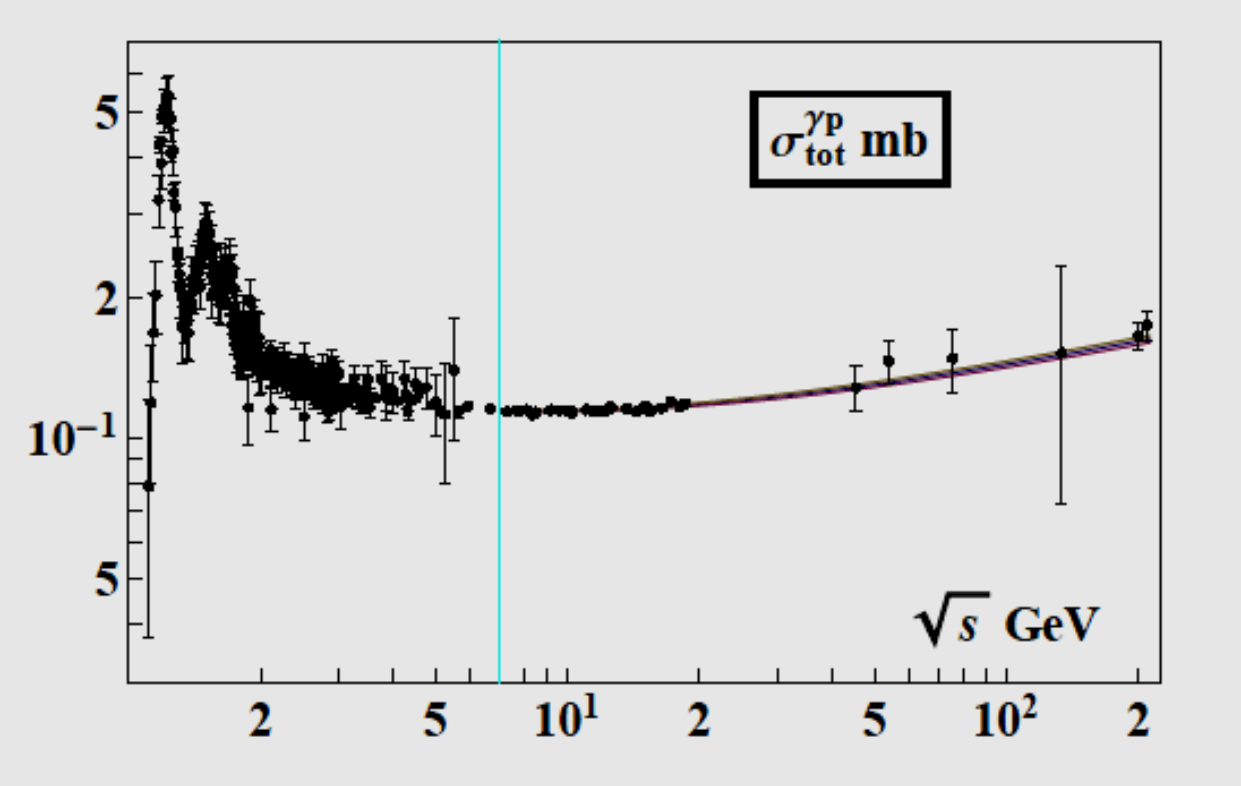

Μοντέλο

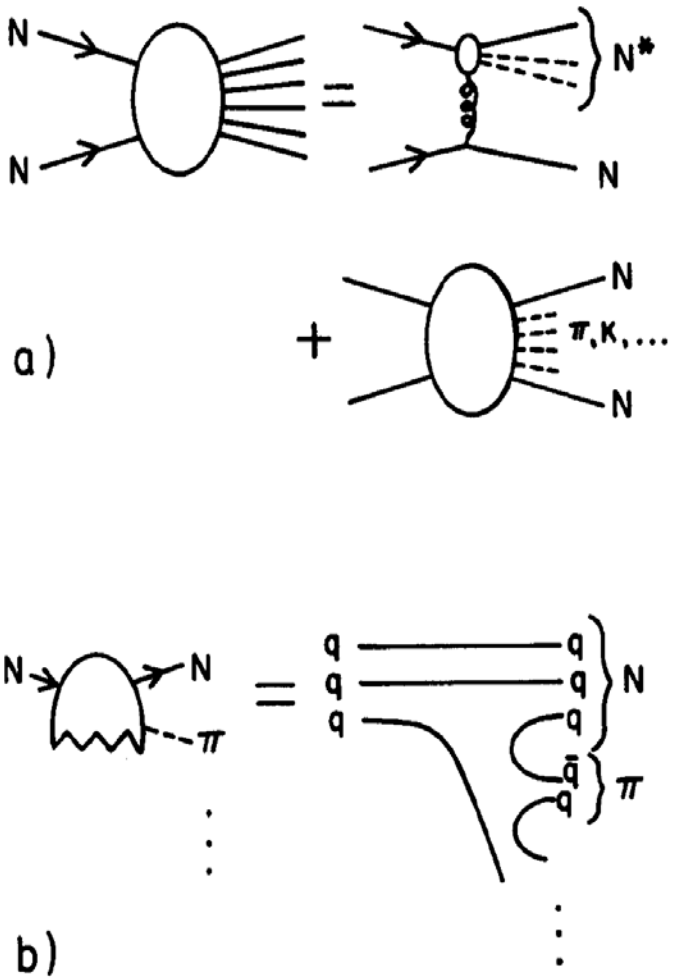

Figure 5.1: (a) Isobar-pionization picture of a nucleon–nucleon collision. (b) Fragmentation of a projectile nucleon.

Μεταβλητές.

Μεταβλητή	Ορισμός	Περιγραφή
x^*	$\frac{p_{\parallel}^*}{p_{\parallel}^*} \cong \frac{2p_{\parallel}^*}{\sqrt{s}}$	Feynman x
x_R	$\frac{E^*}{E_{max}^*} \cong 2\frac{E^*}{\sqrt{s}}$	radial x
μ_T	$\sqrt{p_T^2 + m_c^2}$	transverse mass
$x_{lab}=x_L$	$E_{lab}/E_{lab(max)}$	$= E_{lab}/E_{beam}$
y	$E^* \mu_T \cosh y$	rapidity
η	-ln tan½θ	pseudorapidity

λίγα για την πολλαπλότητα των δευτερογενών

2.1. Feynman Scaling

Feynman concluded that for asymptotically large energies the mean total number of any kind of particle rises logarithmically with $\sqrt{s}$ [20]:

$$\langle N \rangle \propto \ln W \propto \ln \sqrt{s} \quad \text{with} \quad W = \sqrt{s}/2. \tag{1}$$

His conclusions are based on phenomenological arguments about the exchange of quantum numbers between the colliding particles. He argued that the number of particles with a given mass and transverse momentum per longitudinal momentum interval p_z depends on the energy $E = E(p_z)$ as

$$\frac{\mathrm{d}N}{\mathrm{d}p_z} \sim \frac{1}{E}. \tag{2}$$

This was extended to the probability of finding a particle of kind i with mass m and transverse and longitudinal momentum p_T and p_z:

$$f_i(p_T, x_F = p_z/W)\frac{\mathrm{d}p_z}{E}\mathrm{d}^2p_T \tag{3}$$

with the energy of the particle

$$E = \sqrt{m^2 + p_T^2 + p_z^2}. \tag{4}$$

The function $f_i(p_T, x_F)$ denotes the particle distribution. Feynman's hypothesis is that f_i becomes independent of W at high energies. This assumption is known as *Feynman scaling* and f_i is called the scaling function or Feynman function. The variable $x_F = p_z/W$, called *Feynman-x*, is the ratio of the longitudinal momentum of the particle p_z to the total energy of an incident particle W. Integration of expression (3) results in $\langle N \rangle \propto \ln W$. A derivation is given in Appendix A.

Considering that the maximum rapidity in a collisions increases also with $\ln \sqrt{s}$, it follows that:

$$\frac{\mathrm{d}N}{\mathrm{d}y} = \text{constant}, \tag{5}$$

i.e., the height of the rapidity distribution around mid-rapidity, the so-called plateau, is independent of $\sqrt{s}$. Equivalently, the pseudorapidity at mid-rapidity $\mathrm{d}N/\mathrm{d}\eta|_{\eta=0}$ is approximately constant if Feynman scaling holds (the pseudorapidity is defined as $\eta = (1/2)\ln[(p + p_L)/(p - p_L)] = -\ln\tan\vartheta/2$ where p (p_L) is the total (longitudinal)

momentum of the particle and ϑ the angle between the particle and the beam axis). Here the transformation from y to η has to be taken into account. It depends on the average $m_T = \sqrt{m^2 + p_T^2}$ of the considered particles which, however, is only weakly energy-dependent. An estimate based on the Pythia event generator shows that the ratio $(\mathrm{d}N_{\mathrm{ch}}/\mathrm{d}y)/(\mathrm{d}N_{\mathrm{ch}}/\mathrm{d}\eta)$ changes by only 1 – 2% from $\sqrt{s} = 100\,\mathrm{GeV}$ to $1\,\mathrm{TeV}$. Furthermore, this transformation causes a dip in the distribution around $\eta \approx 0$ which is not present in the rapidity distribution itself (see Section 3.4 where measured $\mathrm{d}N_{\mathrm{ch}}/\mathrm{d}\eta$ distributions are shown).

Από το άρθρο:

Charged-Particle Multiplicity in Proton–Proton Collisions

Jan Fiete Grosse-Oetringhaus1, Klaus Reygers2

http://arxiv.org/abs/0912.0023v2

Κατανομές δευτερογενών

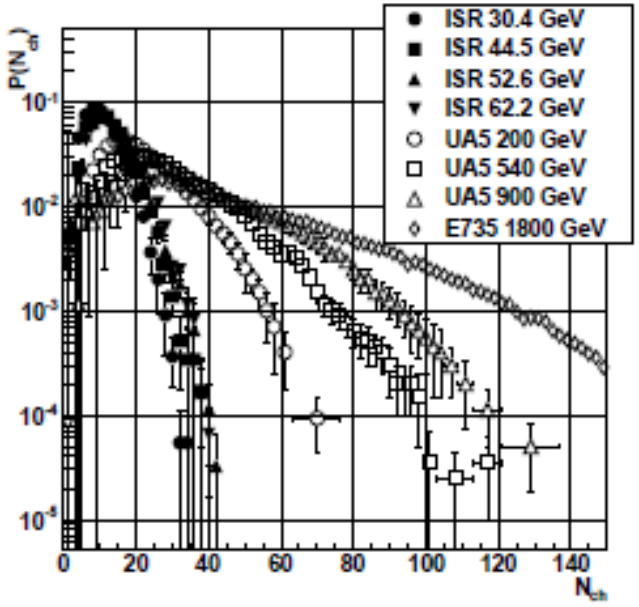

Αριθμός φορτισμένων για διαφορετικές ενέργειες CM

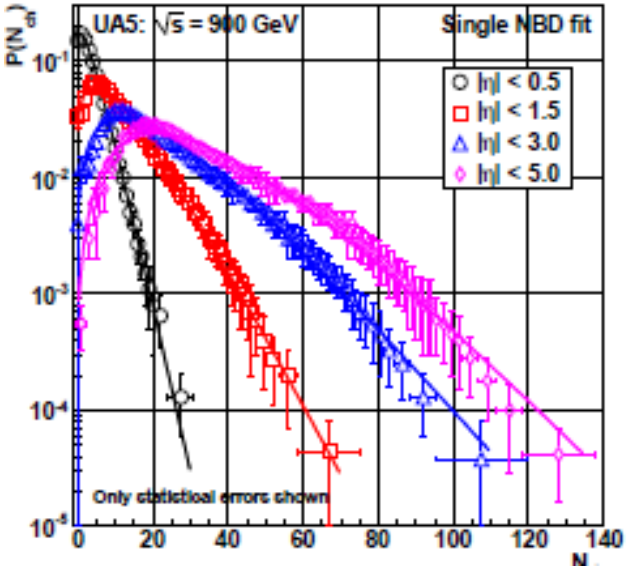

Η πολλαπλότητα ελαττώνεται σημαντικά για μικρές τιμές του η

Μικρή τιμή του η έχουν τα σωματίδια κοντά στη δέσμη.

Μέση πολλαπλότητα σαν συνάρτηση της Εν. CM

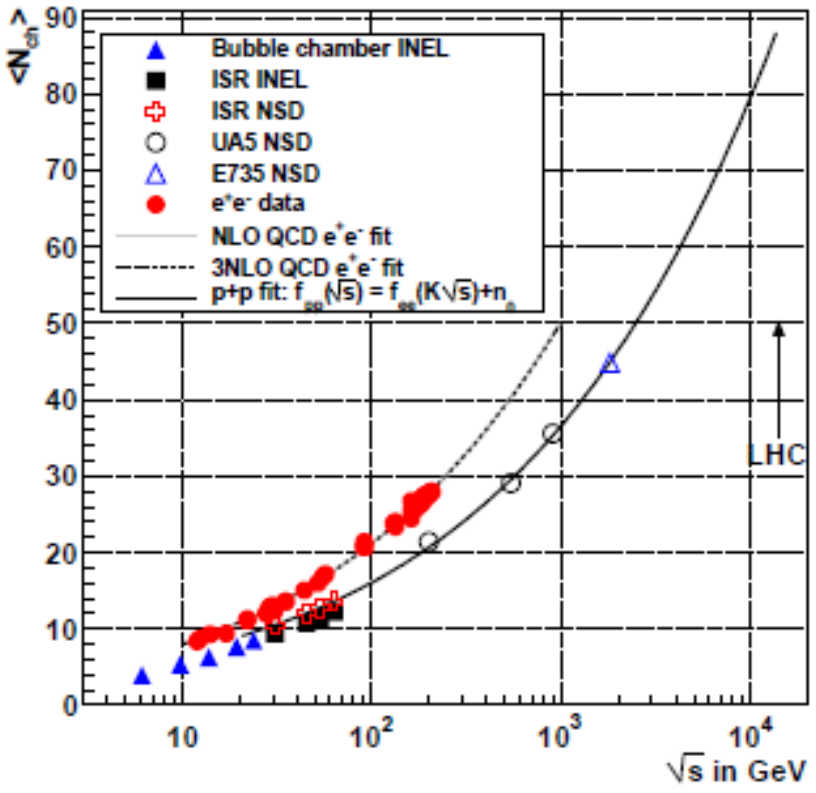

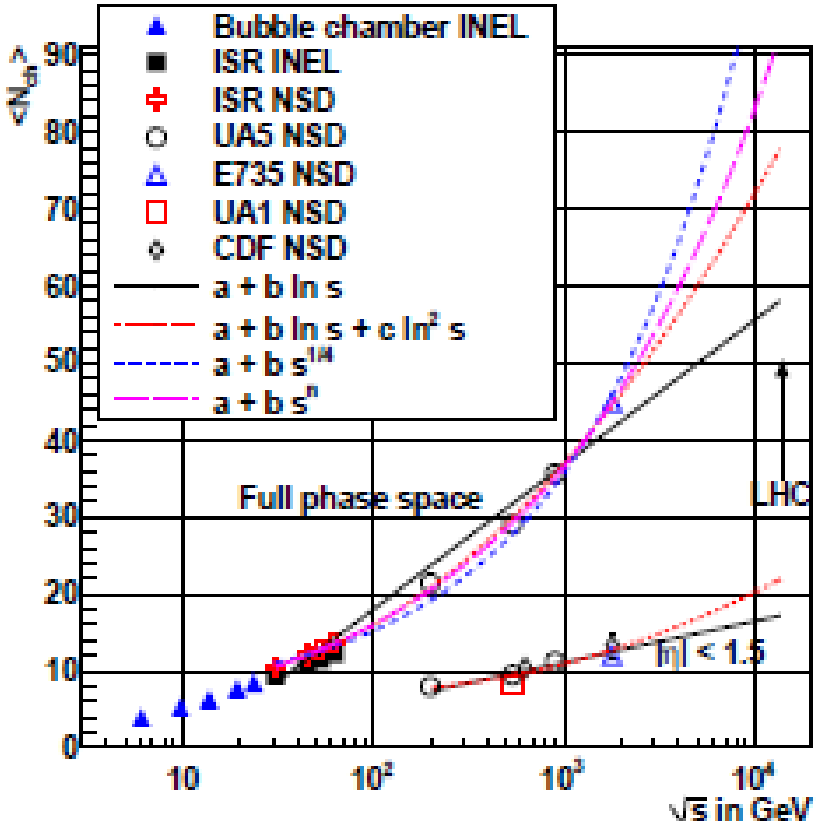

Ανελαστικότητα K (inelasticity)

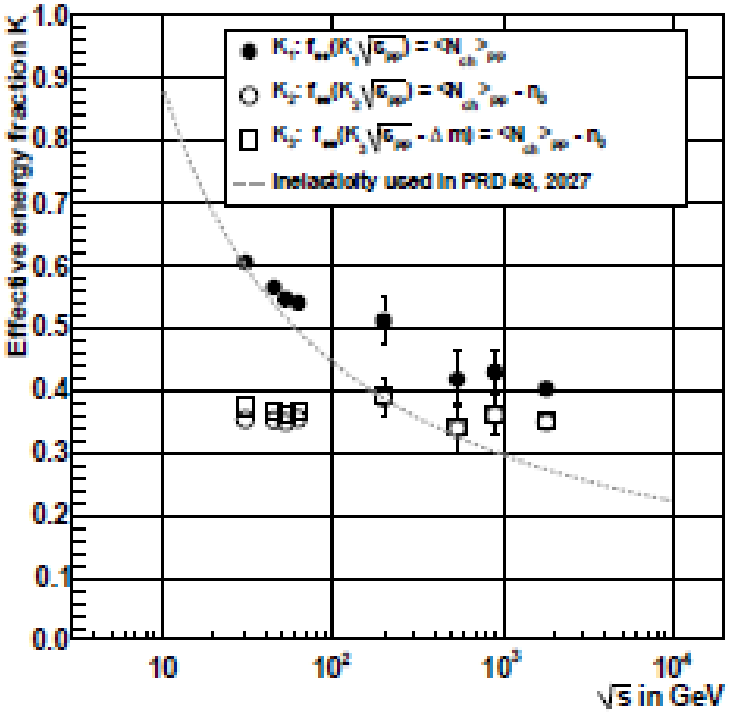

Το ποσοστό ενέργειας της δέσμης που πηγαίνει στα «θραύσματα» (fragmentation). Η υπόλοιπη πηγαίνει στο leading particle.

neutrino parameters

Observed values of oscillation parameters

- $\sin^2(2\theta_{13}) = 0.092 \pm 0.017$[15]
- $\tan^2(\theta_{12}) = 0.457^{+0.040}_{-0.029}$. This corresponds to $\theta_{12} \equiv \theta_{sol} = 34.06^{+1.16}_{-0.84}°$ ("sol" stands for solar)[16]
- $\sin^2(2\theta_{23}) > 0.92$ at 90% confidence level, corresponding to $\theta_{23} \equiv \theta_{atm} = 45 \pm 7.1°$ ("atm" stands for atmospheric)[16]
- $\Delta m^2_{21} \equiv \Delta m^2_{sol} = 7.59^{+0.20}_{-0.21} \times 10^{-5}$ eV^2[16]
- $|\Delta m^2_{31}| \approx |\Delta m^2_{32}| \equiv \Delta m^2_{atm} = 2.43^{+0.13}_{-0.13} \times 10^{-3}$ eV^2[16]
- δ, α_1, α_2, and the sign of Δm^2_{32} are currently unknown

Solar neutrino experiments combined with KamLAND have measured the so-called solar parameters Δm^2_{sol} and $\sin^2\theta_{sol}$. Atmospheric neutrino experiments such as Super-Kamiokande together with the K2K and MINOS long baseline accelerator neutrino experiment have determined the so-called atmospheric parameters Δm^2_{atm} and $\sin^2\theta_{atm}$. The last mixing angle, θ_{13}, has been measured by the Daya Bay Experiment and the RENO as $\sin^2 2\theta_{13}$.
For atmospheric neutrinos (where the relevant difference of masses is about $\Delta m^2 = 2.4 \times 10^{-3}$ eV^2 and the typical energies are ~1 GeV), oscillations become visible for neutrinos traveling several hundred km, which means neutrinos that reach the detector from below the horizon.
The mixing parameter $\sin^2 2\theta_{13}$ is measured using electron anti-neutrinos from nuclear reactors. The rate of anti-neutrino interactions is measured in detectors sited near the reactors to determine the flux prior to any significant oscillations and then it is measured in far detectors (sited about 2 km from the reactors). The oscillation is observed as an apparent disappearance of electron anti-neutrinos in the far detectors (*i.e.* the interaction rate at the far site is lower than predicted from the observed rate at the near site).

Πειράματα Νετρίνων

Σε συντομία οι τρόποι με τους οποίους τα νετρίνα αλληλεπιδρούν με την ύλη.

Αντιδράσεις ουδετέρων ρευμάτων:
μέσω ενός μποζονίου Z
Αντιδράσεις φορτισμένων ρευμάτων
μέσω ενός μποζονίου W και παραγωγή φορτισμένου σωματιδίου

Επίσης σωματίδιο στόχου:

Ατομικό ηλεκτρόνιο
Νουκλεόνιο του πυρήνα.

Φορτισμένο ρεύμα:

Στα διαγράμματα σημειώστε W^-

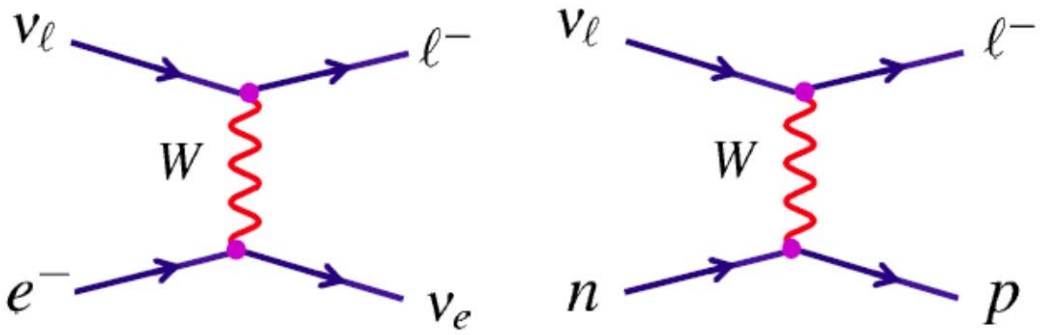

Ουδέτερο ρεύμα.

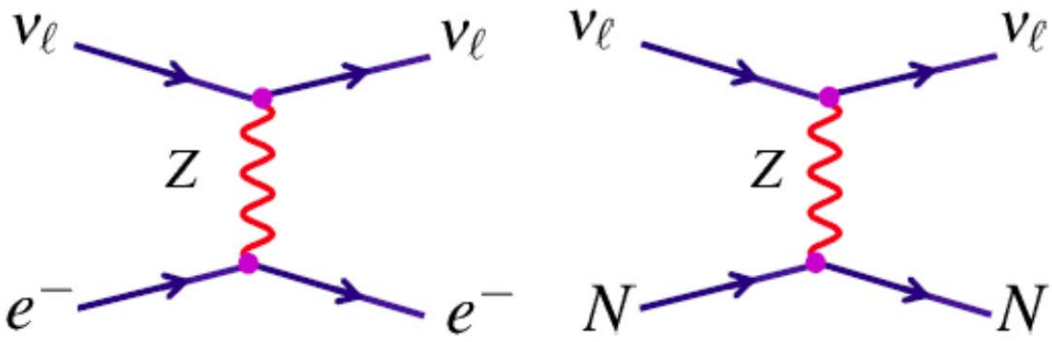

Η μέθοδος ανίχνευσης εξαρτάται από την ενέργεια και το άρωμα του νετρίνου.

Τα ηλιακά νετρίνα έχουν ενέργεια τάξης $E \approx 1$ MeV
Τα κοσμικά έχουν ενέργεια $E \approx 1$ GeV

Οι ενέργειες είναι χαμηλές και δεν είναι επιτρεπτές οι αντιδράσεις όπου χρειάζεται να παραχθεί ένα λεπτόνιο μεγάλης μάζας.

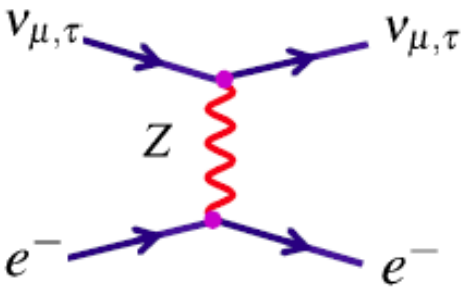

Αντιδράσεις **φορτισμένων ρευμάτων σε ατομικά ηλεκτρόνια.** (Σύστημα εργαστηρίου)
Στο δεξί μέρος του διαγράμματος εμφανίζεται το αντίστοιχο φορτισμένο λεπτόνιο. δηλ αν πέφτει ν_e τότε e^- αν ν_μ τότε μ αν ν_τ τότε τ. Όμως πρέπει να έχει αρκετή ενέργεια για να δημιουργήσει την μάζα του ο υπολογισμός δίνει

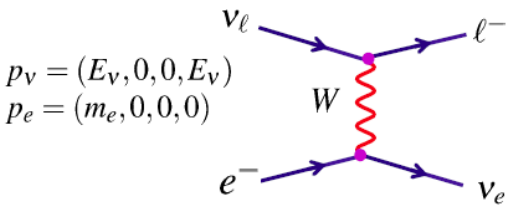

$p_\nu = (E_\nu, 0, 0, E_\nu)$
$p_e = (m_e, 0, 0, 0)$

$$s = (p_\nu + p_e)^2 = (E_\nu + m_e)^2 - E_\nu^2$$

Require: $s > m_\ell^2$

$$\Rightarrow \quad E_\nu > \left[\left(\frac{m_\ell}{m_e}\right)^2 - 1\right]\frac{m_e}{2}$$

$\nu_e + e^- \rightarrow e^- + \nu_e$
$\nu_\mu + e^- \rightarrow \mu^- + \nu_e$
$\nu_\tau + e^- \rightarrow \tau^- + \nu_e$

Με αριθμητική αντικατάσταση:

$$E_{\nu_e} > 0 \qquad E_{\nu_\mu} > 11\,\text{GeV} \qquad E_{\nu_\tau} > 3090\,\text{GeV}$$

Υψηλό κατώφλι για ηλιακά ή ατμοσφαιρικά.

Αντιδράσεις **φορτισμένων ρευμάτων σε νουκλεόνια**. (Σύστημα εργαστηρίου)
Οι συνθήκες είναι πιο ευνοϊκές λόγω της μαζας του νουλεονίου. Οι διατομές εξαρτώνται από τις συναρτήσεις δομής των νουκλεονίων.

για νετρόνια:
Για ν_e αναγνωρίζουμε την αντίστροφη της διάσπασης β.

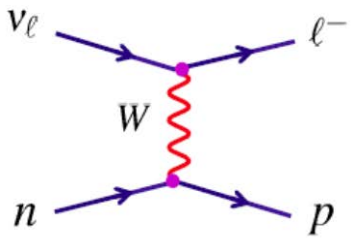

$$s = (p_\nu + p_n)^2 = (E_\nu + m_n)^2 - E_\nu^2$$

Require: $s > (m_\ell + m_p)^2$

$$\Rightarrow \quad E_\nu > \frac{(m_p^2 - m_n^2) + m_\ell^2 + 2m_p m_\ell}{2m_n}$$

$\nu_e + n \rightarrow e^- + p$
$\nu_\mu + n \rightarrow \mu^- + p$
$\nu_\tau + n \rightarrow \tau^- + p$

$$E_{\nu_e} > 0 \qquad E_{\nu_\mu} > 110\,\text{MeV} \qquad E_{\nu_\tau} > 3.5\,\text{GeV}$$

Τα ηλεκτρονιακά νετρίνα από τον ήλιο ή από αντιδραστήρες που **ταλαντώνονται** σε μιονιακά δεν μπορούν να αντιδράσουν επειδή δεν έχουν την απαραίτητη ενέργεια να παράγουν μιόνια και "εξαφανίζονται". (νe --> νμ και Ενμ < 110 MeV)
Αντιδρούν τα ατμοσφαιρικά.
Τα μιονικά νετρίνα που **ταλαντώνονται** σε νετρίνα ταυ επίσης εξαφανίζονται.
Τα περισσότερα πειράματα είναι πειράματα εξαφάνισης (εκτός από το SNO) γιατί η ενέργεια στο σύστημα K.M , είναι κάτω από το κατώφλι για παραγωγή λεπτονίου με διαφορετικό άρωμα όπως γαίνεται από τις .
Για μιονικά νετρίνα υψηλής ενέργειας ισχύει :

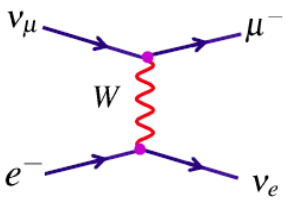

$$\sigma_{\nu_\mu e^-} = \frac{G_F^2 s}{\pi}$$

with $\quad s = (E_\nu + m_e)^2 - E_\nu^2 \approx 2 m_e E_\nu$

$$\sigma_{\nu_\mu e^-} = \frac{2 m_e G_F^2 E_\nu}{\pi}$$

Cross section increases linearly with lab. frame neutrino energy

Για ηλεκτρονιακά νετρίνα για την ίδια τελική κατάσταση έχουμε τα διαγράμματα:

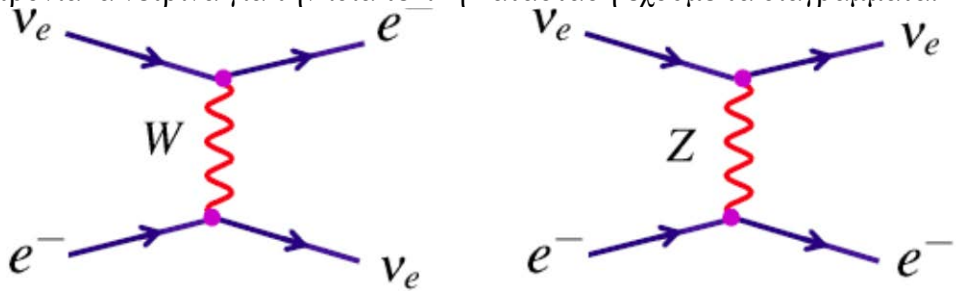

Η συνολική ενεργή διατομή είναι μικρότερη από σκέτη φορτισμένων ρευμάτων λόγω αρνητικής συμβολής των δύο διαγραμμάτων.

$$\sigma_{\nu_e e} \approx 0.6 \sigma^{CC}_{\nu_e e}$$

Στις υψηλές ενέργειες η διατομές νετρίνο νουκλεόνιο είναι μεγαλύτερες λόγω της υψηλότερης διαθέσιμης ενέργειας στο KM.

$$s = (E_\nu + m_n)^2 - E_\nu^2 \approx 2 m_n E_\nu$$

Neutrino Detection

★ The detector technology/interaction process depends on type of neutrino and energy

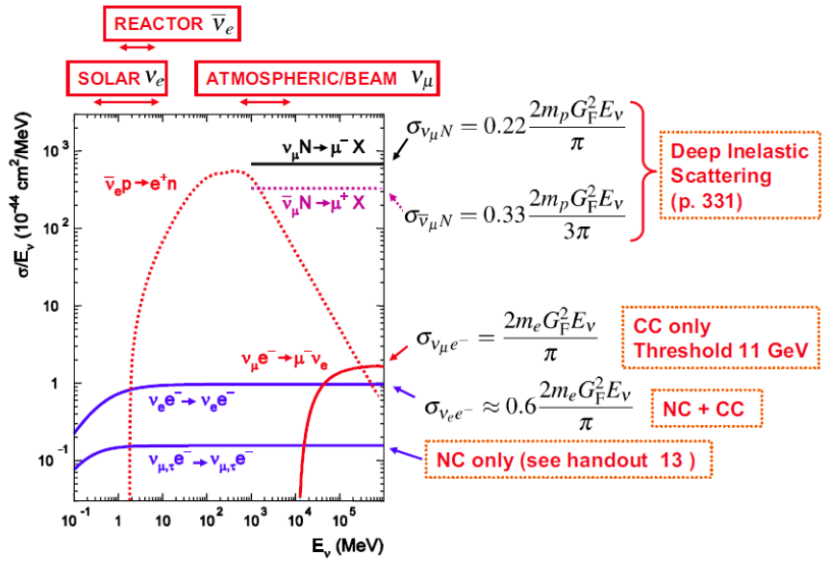

Τα ηλιακά νετρίνα ανιχνεύονται την αντίστροφη β .

Τα ατμοσφαιρικά ανιχνεύονται από την βαθιά ανελαστική σκέδαση. Η σκέδαση στα ηλεκτρόνια συνεισφέρει σε πολύ μικρό ποσοστό.

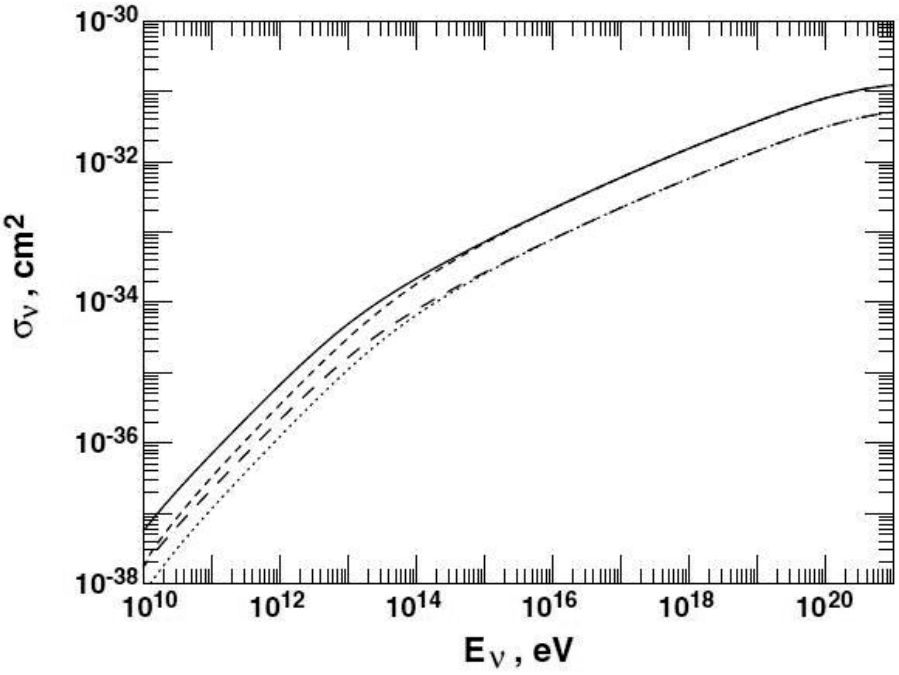

Fig. 10.2. Cross-sections for deep inelastic neutrino scattering. Neutrino CC cross-section is plotted with a solid line, the antineutrino with short dashes. The NC cross-section for neutrinos are plotted with long dashes, and for antineutrinos with a dotted line.

Στις χαμηλές ενέργειες η ενεργός διατομή των αντι-νετρίνων είναι περίπου το 1/3 των νετρίνων.

1 GeV $\sigma\, \nu^- \cong 1/3\, \sigma\, \nu$ 100 GeV$\cong \sigma\, \nu$

Οι διατομές των ουδετέρων ρευμάτων είναι περίπου οι μισές από τις αντίστοιχες των φορτισμένων.

Το σημείο καμπής αντιστοιχεί στην ενέργεια εργαστηρίου που χρειάζεται για την παραγωγή του W και του Z αντίστοιχα.

Συντονισμός Glashow

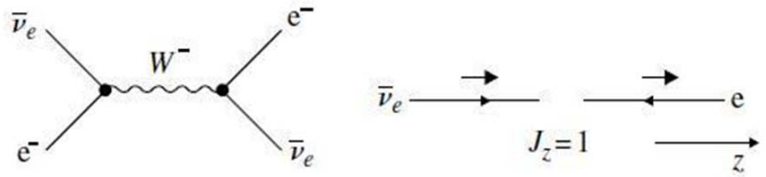

Η σκέδαση του αντι ν_e σε ηλεκτρόνιο γίνεται με την μεσολάβηση ενός μποζονίου W^-. Στον τύπο της ενεργής διατομής εμφανίζεται ο όρος

$$\left(1-\frac{2m_eE_\nu}{M_w}\right)^{-2}$$

Η διατομή μεγιστοποιείται όταν η ενέργεια του νετρίνου γίνει ίση με 6.4 PeV δηλαδή μπορεί να παράγει την μάζα του W. Η διαθέσιμη ενέργεια στο ΚΜ είναι :

$$\sqrt{s} = 2m_eE_\nu$$

Η διατομή στην ενέργεια αυτή , είναι περίπου 300 φορές μεγαλύτερη από το άθροισμα των διατομών όλων των άλλων αντιδράσεων.
Στις άλλες αντιδράσεις των νετρίνων δεν εμφανίζεται ό όρος αυτός λόγω διαφορετικού συνδυασμού των spin.
Στην τελική κατάταση έχουμε τα προιόντα της διασπασης του W
Δηλαδή:

$W^+ \rightarrow \nu_l$ + hadrons 68%
$\rightarrow \nu_e$ +e 10,5%
$\rightarrow \nu_\mu + \mu$ 10,5%
$\rightarrow \nu_\tau + \tau$ 11%

Το ηλεκτρόνιο που παράγεται δημιουργεί πάντοτε Η.Μ. καταιονισμό τον οποίο μπορούμε να ανιχνεύσουμε. Στον καταιονισμό πηγαίνει σχεδόν το 100% της ενέρειας του νετρίνου. Το μήκος του καταιοινισμού για νετρίνο 1 PeV είναι περίπου 7 m .
Τα αδρόνια δημιουργούν αδρονικό καταιονισμό του οποίου η ενέργεια είναι περίπου 50% της αρχικής.
Το μιόνιο δημιουργεί μία τροχιά την οποία ανιχνεύουμε από το φως Τσερένκωφ.
Το τ δημιουργεί αδρονικό καταιονισμό.

(D. Perkins σελ. 68, S. L. Glashow Phys. Rev 118 (1960) 316-317)

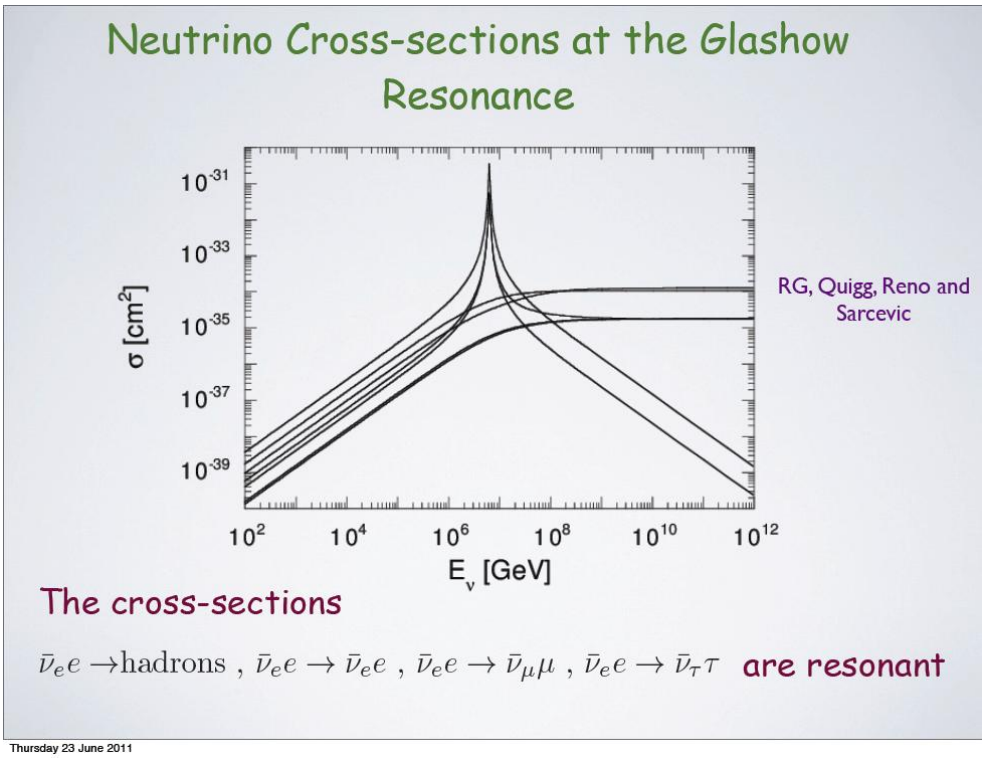

Ενεργός διατομή σαν συνάρτηση της ενέργειας, συντονισμός Glashow.

Αντιδράσεις σε συντονισμό.

Interaction	$\sigma\,[\mathrm{cm}^2]$
$\bar{\nu}_e\, e \rightarrow \bar{\nu}_e e$	5.38×10^{-32}
$\bar{\nu}_e\, e \rightarrow \bar{\nu}_\mu \mu$	5.38×10^{-32}
$\bar{\nu}_e\, e \rightarrow$ hadrons	3.41×10^{-31}
$\bar{\nu}_e\, e \rightarrow$ anything	**5.02×10^{-31}**

Αντιδράσεις εκτός συντονισού.

Interaction	$\sigma\,[\mathrm{cm}^2]$
$\nu_\mu N \rightarrow \mu$ + anything	**1.43×10^{-33}**
$\nu_\mu N \rightarrow \nu_\mu$ + anything	6.04×10^{-34}
$\nu_\mu e \rightarrow \nu_e + \mu$	5.42×10^{-35}

Παρατηρούμε την διαφορά σε τάξεις μεγέθους.

Το ηλεκτρόνιο που παράγεται δημιουργει Η.Μ. καταιονισμό τον οποίο ανιχνεύουμε.

★ Electron neutrinos from the sun and nuclear reactors $E_\nu \sim 1\,\mathrm{MeV}$ which oscillate into muon or tau neutrinos cannot interact via charged current interactions – "they effectively disappear"

★ Atmospheric muon neutrinos $E_\nu \sim 1\,\mathrm{GeV}$ which oscillate into tau neutrinos cannot interact via charged current interactions – "disappear"

•To date, most experimental signatures for neutrino oscillation are a deficit of neutrino interactions (with the exception of SNO) because below threshold for produce lepton of different flavour from original neutrino

•In Handout 10 derived expressions for CC neutrino-quark cross sections in ultra-relativistic limit (neglecting masses of neutrinos/quarks)

•For high energy muon neutrinos can directly use the results from page 316

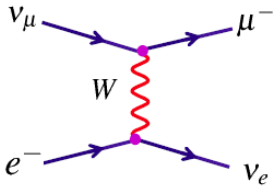

$$\sigma_{\nu_\mu e^-} = \frac{G_F^2 s}{\pi}$$

with $s = (E_\nu + m_e)^2 - E_\nu^2 \approx 2m_e E_\nu$

$$\sigma_{\nu_\mu e^-} = \frac{2m_e G_F^2 E_\nu}{\pi}$$

Cross section increases linearly with lab. frame neutrino energy

•For electron neutrinos there is another lowest order diagram with the same final state

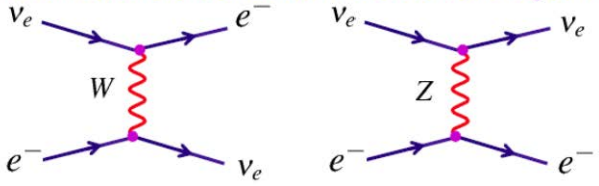

It turns out that the cross section is lower than the pure CC cross section due to negative interference when summing matrix elements $|M_{CC} + M_{NC}|^2 < |M_{CC}|^2$

$$\sigma_{\nu_e e} \approx 0.6\sigma_{\nu_e e}^{CC}$$

•In the high energy limit the CC neutrino-nucleon cross sections are larger due to the higher centre-of-mass energy: $s = (E_\nu + m_n)^2 - E_\nu^2 \approx 2m_n E_\nu$

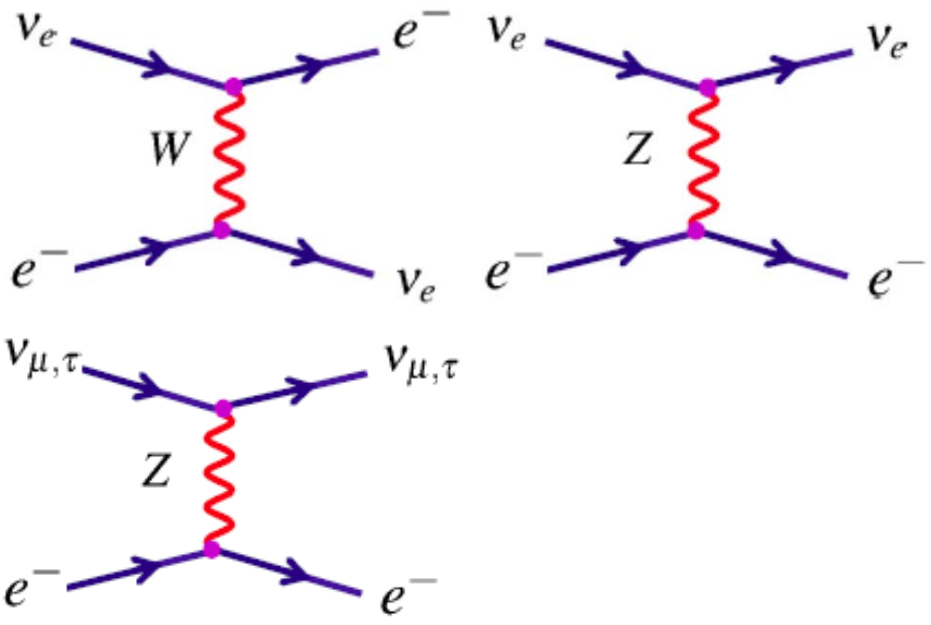

Inverse Compton Scattering

Comptonisation is a vast subject. *Inverse Compton scattering* involves the scattering of low energy photons to high energies by ultrarelativistic electrons so that the photons gain and the electrons lose energy. The process is called *inverse* because the electrons lose energy rather than the photons, the opposite of the standard Compton effect. We will treat the case in which the energy of the photon in the centre of momentum frame of the interaction is much less that $m_{\rm e}c^2$, and consequently the Thomson scattering cross-section can be used to describe the probability of scattering.

Many of the most important results can be worked out using simple physical arguments, as for example in Blumenthal and Gould (1970) and Rybicki and Lightman (1979).

Inverse Compton Scattering

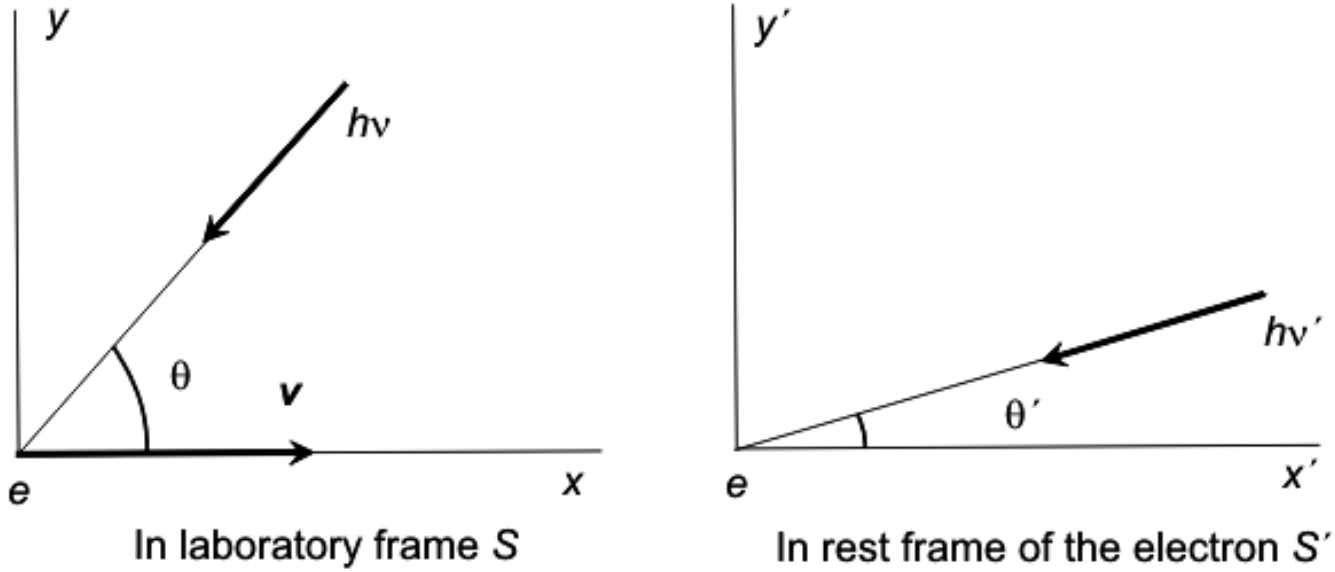

Consider a collision between a photon and a relativistic electron as seen in the laboratory frame of reference S and in the rest frame of the electron S′. Since $\hbar\omega' \ll m_e c^2$ in S′, the centre of momentum frame is very closely that of the relativistic electron. If the energy of the photon is $\hbar\omega$ and the angle of incidence θ in S, its energy in the frame S′ is

$$\hbar\omega' = \gamma\hbar\omega[1 + (v/c)\cos\theta] \qquad (1)$$

according to the standard relativistic Doppler shift formula.

Inverse Compton Scattering

Similarly, the angle of incidence θ' in the frame S$'$ is related to θ by the formulae

$$\sin\theta' = \frac{\sin\theta}{\gamma[1+(v/c)\cos\theta]} \quad ; \quad \cos\theta' = \frac{\cos\theta + v/c}{1+(v/c)\cos\theta}. \tag{2}$$

Now, provided $\hbar\omega' \ll m_{\rm e}c^2$, the Compton interaction in the rest frame of the electron is simply Thomson scattering and hence the energy loss rate of the electron in S$'$ is just the rate at which energy is reradiated by the electron.

According to the analysis of Thomson scattering (22, Lecture 1), the loss rate is

$$-({\rm d}E/{\rm d}t)' = \sigma_{\rm T} c U'_{\rm rad}, \tag{3}$$

where $U_{\rm rad}$ is the energy density of radiation in the rest frame of the electron. As discussed in that section, it is of no importance whether or not the radiation is isotropic. The free electron oscillates in response to any incident radiation field. Our strategy is therefore to work out $U'_{\rm rad}$ in the frame of the electron S$'$ and then to use (3) to work out $({\rm d}E/{\rm d}t)'$. Because ${\rm d}E/{\rm d}t$ is an invariant between inertial frames, this is also the loss rate $({\rm d}E/{\rm d}t)$ in the observer's frame S.

Working out U'_{rad} in S′

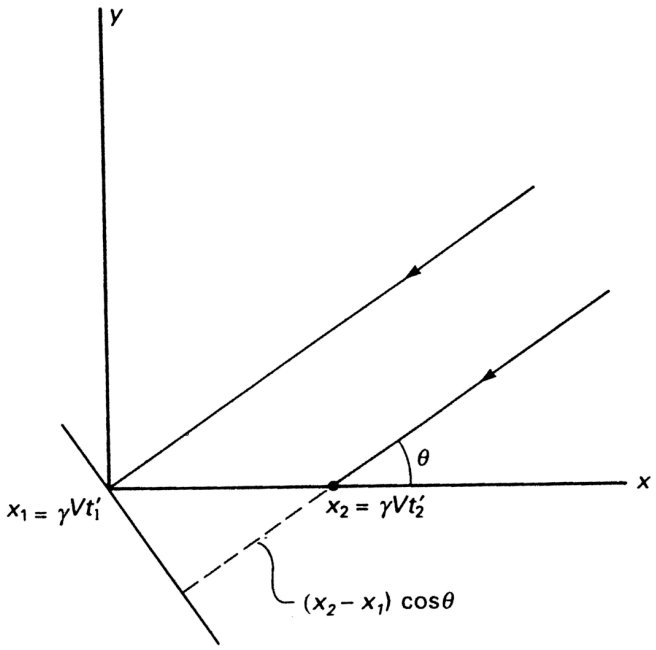

In S, the electron moves from x_1 to x_2 in the time interval t_1 to t_2. These are transformed into S′ by the standard Lorentz transformation

Suppose the number density of photons in a beam of radiation incident at angle θ to the x-axis is N. Then, the energy density of these photons in S is $N\hbar\omega$. The flux density of photons incident upon an electron stationary in S is $U_{\text{rad}}c = N\hbar\omega c$.

Now let us work out the flux density of this beam in the frame of reference of the electron S′. We need two things, the energy of each photon in S′ and the rate of arrival of these photons at the electron in S′. The first of these is given by (3). The second factor requires a little bit of care, although the answer is obvious in the end. The beam of photons incident at angle θ in S arrives at an angle θ' in S′ according to the aberration formulae (2).

Working out U'_{rad} in S′

We are interested in the rate of arrival of photons at the origin of S′ and so let us consider two photons which arrive there at times t'_1 and t'_2. The coordinates of these events in S are

$$[x_1, 0, 0, t_1] = [\gamma V t'_1, 0, 0, \gamma t'_1] \quad \text{and} \quad [x_2, 0, 0, t_2] = [\gamma V t'_2, 0, 0, \gamma t'_2] \qquad (4)$$

respectively. This calculation makes the important point that the photons in the beam are propagated along parallel but separate trajectories in S as illustrated by Fig. 30. From the geometry of the figure, it is apparent that the time difference when the photons arrive at a plane perpendicular to their direction of propagation in S is

$$\Delta t = t_2 + \frac{(x_2 - x_1)}{c}\cos\theta - t_1 = (t'_2 - t'_1)\gamma[1 + (v/c)\cos\theta], \qquad (5)$$

that is, the time interval between the arrival of photons from the direction θ is shorter by a factor $\gamma[1 + (v/c)\cos\theta]$ in S′ than it is in S.

Working out U'_{rad} in S′

Thus, the rate of arrival of photons, and correspondingly their number density, is greater by this factor $\gamma[1 + (v/c)\cos\theta]$ in S′ as compared with S. This is exactly the same factor by which the energy of the photon has increased (3). On reflection, we should not be surprised by this result because these are two different aspects of the same relativistic transformation between the frames S and S′, in one case the frequency interval and, in the other, the time interval.

Thus, as observed in S′, the energy density of the beam is therefore

$$U'_{\mathrm{rad}} = [\gamma(1 + (v/c)\cos\theta)]^2\, U_{\mathrm{rad}}. \tag{6}$$

Now, this energy density is associated with the photons incident at angle θ in the frame S and consequently arrives within solid angle $2\pi \sin\theta\, \mathrm{d}\theta$ in S. We assume that the radiation field in S is isotropic and therefore we can now work out the total energy density seen by the electron in S′ by integrating over solid angle in S, that is,

$$U'_{\mathrm{rad}} = U_{\mathrm{rad}} \int_0^{\pi} \gamma^2 [1 + (v/c)\cos\theta]^2\, \tfrac{1}{2} \sin\theta\, \mathrm{d}\theta. \tag{7}$$

The Inverse Compton Energy Loss Rate

Integrating, we find

$$U'_{\rm rad} = \tfrac{4}{3} U_{\rm rad} (\gamma^2 - \tfrac{1}{4}). \tag{8}$$

Therefore, substituting into (3), we find

$$({\rm d}E/{\rm d}t)' = ({\rm d}E/{\rm d}t) = \tfrac{4}{3} \sigma_{\rm T} c U_{\rm rad} (\gamma^2 - \tfrac{1}{4}). \tag{9}$$

Now, this is the energy gained by the photon field due to the scattering of the low energy photons. We have therefore to subtract the energy of these photons to find the total energy gain to the photon field in S. The rate at which energy is removed from the low energy photon field is $\sigma_{\rm T} c U_{\rm rad}$ and therefore, subtracting, we find

$${\rm d}E/{\rm d}t = \tfrac{4}{3} \sigma_{\rm T} c U_{\rm rad} (\gamma^2 - \tfrac{1}{4}) - \sigma_{\rm T} c U_{\rm rad} = \tfrac{4}{3} \sigma_{\rm T} c U_{\rm rad} (\gamma^2 - 1). \tag{10}$$

We now use the identity $(\gamma^2 - 1) = (v^2/c^2)\gamma^2$ to write the loss rate in its final form

$$\boxed{{\rm d}E/{\rm d}t = \tfrac{4}{3} \sigma_{\rm T} c U_{\rm rad} \left(\frac{v^2}{c^2}\right) \gamma^2.} \tag{11}$$

Synchrotron Radiation and Inverse Compton Losses

This is the remarkably elegant result we have been seeking. It is exact so long as $\gamma\hbar\omega \ll m_{\rm e}c^2$.

Notice the remarkable similarity between the expressions for the loss rates by synchrotron radiation (15) and by inverse Compton scattering (11), even down to the factor of $\frac{4}{3}$ in front of the two expressions.

$$-\left(\frac{{\rm d}E}{{\rm d}t}\right)_{\rm IC} = \tfrac{4}{3}\sigma_{\rm T}cU_{\rm rad}\left(\frac{v^2}{c^2}\right)\gamma^2 \qquad -\left(\frac{{\rm d}E}{{\rm d}t}\right)_{\rm sync} = \tfrac{4}{3}\sigma_{\rm T}cU_{\rm mag}\left(\frac{v}{c}\right)^2\gamma^2 \quad (12)$$

This is not an accident. The reason for the similarity is that, in both cases, the electron is accelerated by the electric field which it observes in its instantaneous rest-frame. The electron does not really care about the origin of the electric field. In the case of synchrotron radiation, the constant accelerating electric field is associated with the motion of the electron through the magnetic field $\boldsymbol{B}$, $\boldsymbol{E}' = \boldsymbol{v}\times\boldsymbol{B}$, and, in the case of inverse Compton scattering, it is the sum of all the electric fields of the incident waves. Notice that, in the latter case, the fields of the waves add incoherently and it is the sum of the squares of the electric field strengths of the waves which appears in the formulae.

The Spectrum of Inverse Compton Radiation

The next calculation is the determination of the spectrum of the scattered radiation. This can be found by performing two successive Lorentz transformations, first transforming the photon distribution into the frame S′ and then transforming the scattered radiation back into the laboratory frame of reference S. This is not a trivial calculation, but the exact result is given by Blumenthal and Gould (1970) for an incident isotropic photon field at a single frequency ν_0. They show that the spectral emissivity $I(\nu)$ may be written

$$I(\nu)\,\mathrm{d}\nu = \frac{3\sigma_{\mathrm{T}}c}{16\gamma^4}\frac{N(\nu_0)}{\nu_0^2}\nu\left[2\nu\ln\left(\frac{\nu}{4\gamma^2\nu_0}\right)+\nu+4\gamma^2\nu_0-\frac{\nu^2}{2\gamma^2\nu_0}\right]\mathrm{d}\nu, \qquad (13)$$

where the radiation field is assumed to be monochromatic with frequency ν_0; $N(\nu_0)$ is the number density of photons. At low frequencies, the term in square brackets in (13) is a constant and hence the scattered radiation has the form $I(\nu) \propto \nu$.

The Spectrum of Inverse Compton Radiation

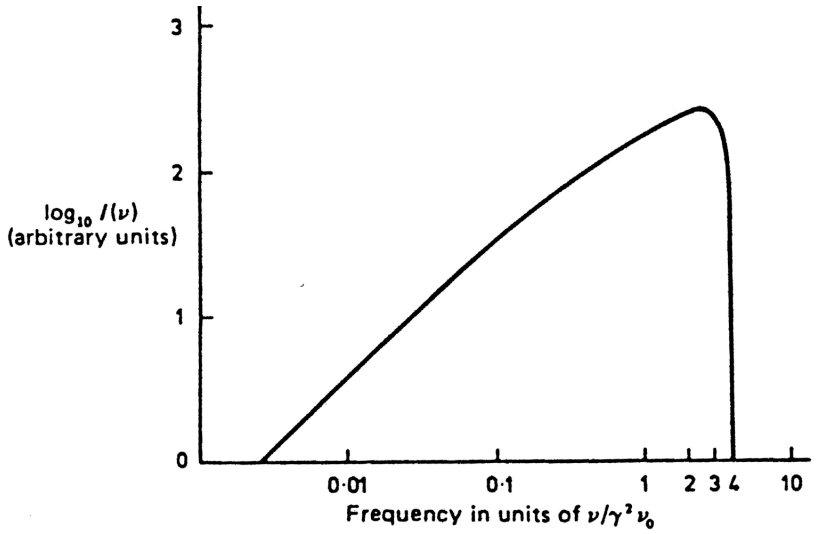

It is an easy calculation to show that the maximum energy which the photon can acquire corresponds to a head-on collision in which the photon is sent back along its original path. The maximum energy of the photon is

$$(\hbar\omega)_{\mathrm{max}} = \hbar\omega\gamma^2(1+v/c)^2 \approx 4\gamma^2\hbar\omega_0. \quad (14)$$

Another interesting result comes out of the formula for the total energy loss rate of the electron (11). The number of photons scattered per unit time is $\sigma_{\mathrm{T}}cU_{\mathrm{rad}}/\hbar\omega_0$ and hence the average energy of the scattered photons is

$$\hbar\omega = \tfrac{4}{3}\gamma^2(v/c)^2\hbar\omega_0 \approx \tfrac{4}{3}\gamma^2\hbar\omega_0. \quad (15)$$

This result gives substance to the hand-waving argument that the photon gains one factor of γ in transforming into S′ and then gains another on transforming back to S.

Inverse Compton Radiation

The general result that the frequency of the scattered photons is $\nu \approx \gamma^2 \nu_0$ is of profound importance in high energy astrophysics. We know that there are electrons with Lorentz factors $\gamma \sim 100 - 1000$ in various types of astronomical source and consequently they scatter any low energy photons to very much higher energies. Consider the scattering of radio, infrared and optical photons scattered by electrons with $\gamma = 1000$.

Waveband	*Frequency (Hz)* ν_0	*Scattered Frequency (Hz) and Waveband*
Radio	10^9	$10^{15} =$ UV
Far-infrared	3×10^{12}	$3 \times 10^{18} =$ X-rays
Optical	4×10^{14}	$4 \times 10^{21} \equiv 1.6$MeV $= \gamma$-rays

Thus, inverse Compton scattering is a means of creating very high energy photons indeed. It also becomes an inevitable drain of energy for high energy electrons whenever they pass through a region in which there is a large energy density of photons.

Emission of a Distribution of Electron Energies

When these formulae are used in astrophysical calculations, it is necessary to integrate over both the spectrum of the incident radiation and the spectrum of the relativistic electrons. The enthusiast is urged to consult the excellent review paper by Blumenthal and Gould (1970). Some of the results are, however, immediately apparent from the close analogy between the inverse Compton scattering and synchrotron radiation processes. For example,the spectrum of the inverse Compton scattering of photons of energy $h\nu$ by a power-law distribution of electron energies

$$\mathrm{d}N \propto E^{-p}\,\mathrm{d}E. \tag{16}$$

results in an intensity spectrum of the scattered radiation of the form

$$I(\nu) \propto \nu^{-(p-1)/2}, \tag{17}$$

because of the γ^2 dependence of the energy loss rate by inverse Compton scattering and the fact that the frequency of the scattered radiation is $\nu \approx \gamma^2 \nu_0$.

Application to Double Radio Sources

The ratio of the total amount of energy liberated by synchrotron radiation and by inverse Compton scattering by the same distribution of electrons is

$$\frac{(\mathrm{d}E/\mathrm{d}t)_{\mathrm{sync}}}{(\mathrm{d}E/\mathrm{d}t)_{\mathrm{IC}}} = \frac{\int I_\nu \,\mathrm{d}\nu \text{ (radio)}}{\int I_X \,\mathrm{d}\nu_X \text{ (X-ray)}} = \frac{B^2/2\mu_0}{U_{\mathrm{rad}}}, \tag{18}$$

where U_{rad} is the energy density of radiation and B the magnetic flux density in the source region. Thus, if we measure the radio and X-ray flux densities from a source region and we know U_{rad}, we can find the magnetic flux density in the source. This type of phenomenon has been sought for in the hot spots and the extended structures of double radio sources. In the latter case, it is likely that the dominant source of low energy photons is the Cosmic Microwave Background Radiation.

Cygnus A

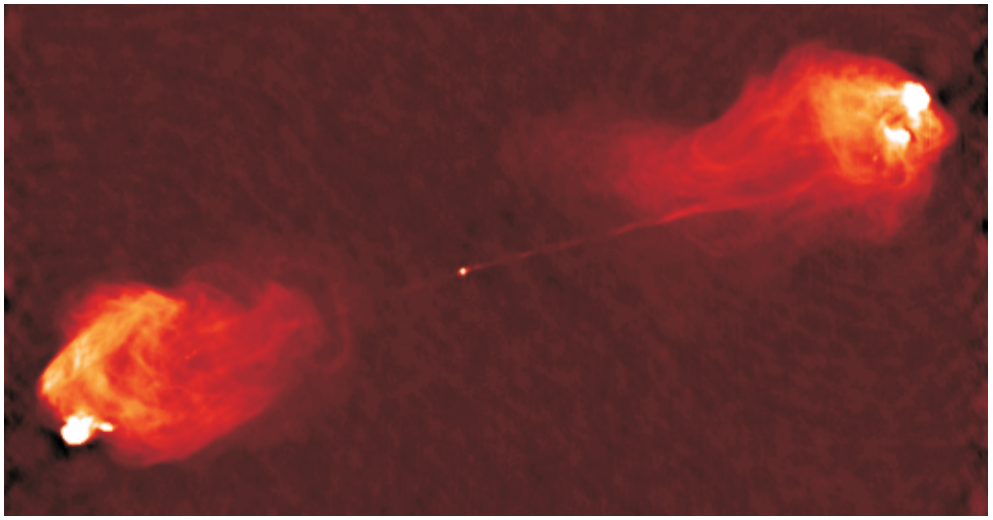

Radio Map from VLA

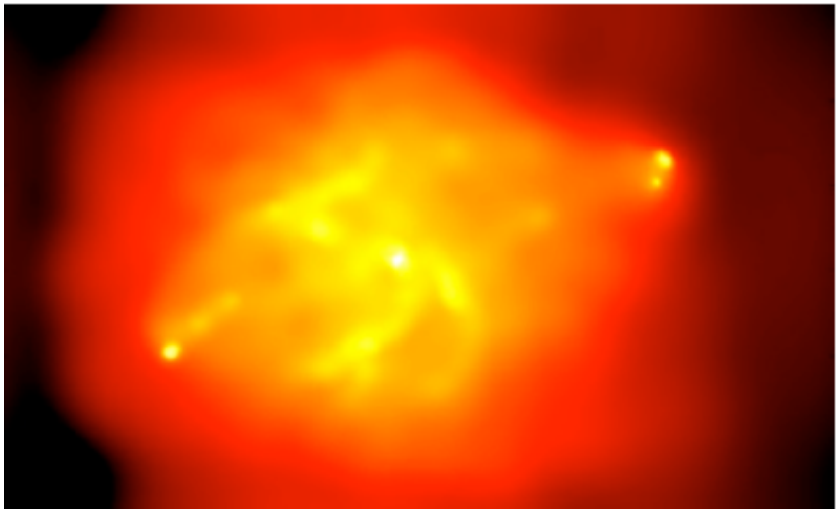

Chandra X-ray Map

The hot-spots of Cygnus A is a good example of this. According to Wilson, Young and Shopbell (2002), if the X-ray hot-spots are identified with inverse Compton scattering of the radio synchrotron emission within the lobes (Synchrotron-self Compton Radiation - see later), the magnetic field strength is 1.5×10^{-4} G. This figure is close to the equipartition value of the magnetic field strengths $2.5 - 2.8 \times 10^{-4}$ G, assuming $\eta = 0$. It is inferred that the relativistic plasma may well be an electron-positron plasma. Similar results are found in hot spots in other double radio sources.

The Maximum Lifetimes of High Energy Electrons

An important piece of astrophysics involving the Cosmic Microwave Background Radiation is that relativistic electrons can never escape from it since it permeates all space. The energy density of the Cosmic Microwave Background Radiation is $U_0 = aT^4 = 2.6 \times 10^5$ eV m^{-3}. Therefore, the maximum lifetime τ of any electron against inverse Compton Scattering is

$$\tau = \frac{E}{|\mathrm{d}E/\mathrm{d}t|} = \frac{E}{\frac{4}{3}\sigma_\mathrm{T} c \gamma^2 U_0} = \frac{2.3 \times 10^{12}}{\gamma} \text{ years} \qquad (19)$$

For example, we observe 100 GeV electrons at the top of the atmosphere and so they must have lifetimes $\tau \leq 10^7$ years.

Synchro-Compton Radiation and the Inverse Compton Catastrophe

Inverse Compton scattering is likely to be an important source of X-rays and γ-rays, for example, in the intense extragalactic γ-ray sources. Wherever there are large number densities of soft photons, the presence of ultrarelativistic electrons must result in the production of high energy photons, X-rays and γ-rays. The case of special interest in this chapter is that in which the same relativistic electrons which are the source of the soft photons are also responsible for scattering these photons to X-ray and γ-ray energies – this is the process known as *synchro-Compton Radiation*. One case of special importance is that in which the number density of low energy photons is so great that most of the energy of the electrons is lost by synchro-Compton radiation rather then by synchotron radiation. This line of reasoning leads to what is known as the *inverse Compton catastrophe*.

Synchro-Compton Catastrophe (for radio astronomers)

The ratio, η, of the rates of loss of energy of an ultrarelativistic electron by inverse Compton and synchrotron radiation in the presence of a photon energy density U_{rad} and a magnetic field of magnetic flux density B is

$$\eta = \frac{(\mathrm{d}E/\mathrm{d}t)_{\mathsf{IC}}}{(\mathrm{d}E/\mathrm{d}t)_{\mathsf{sync}}} = \frac{U_{\mathsf{photon}}}{B^2/2\mu_0}. \tag{20}$$

The synchro-Compton catastrophe occurs if this ratio is greater than 1. In that case, low energy photons, say, radio photons produced by synchrotron radiation, are scattered to X-ray energies by the same flux of relativistic electrons. Since η is greater than 1, the energy density of the X-rays is greater than that of the radio photons and so the electrons suffer an even greater rate of loss of energy by scattering these X-rays to γ-ray energies. In turn, these γ-rays have a greater energy density than the X-rays . . . and so on. It can be seen that as soon as the ratio (20) becomes greater than one, all the energy of the electrons is lost at the very highest energies and so the radio source should instead be a very powerful source of X-rays and γ-rays. Note that for the hot spots of Cygnus A, $\eta \ll 1$.

Synchro-Compton Radiation

Let us study the first stage of the process for the case of compact synchrotron self-absorbed radio sources. We need the energy density of radiation within a synchrotron self-absorbed radio source. As we have shown shown, the flux density of such a source is

$$S_\nu = \frac{2kT_\mathrm{e}}{\lambda^2}\Omega \quad \text{where} \quad \Omega \approx \theta^2 = \frac{r^2}{D^2}. \tag{21}$$

Ω is the solid angle subtended by the source, r is the size of the source and D its distance. For a synchrotron self-absorbed source, the electron temperature of the relativistic electrons is the same as its brightness temperature $T_\mathrm{e} = T_\mathrm{b}$. The radio luminosity of the source is

$$L_\nu = 4\pi D^2 S_\nu = \frac{8\pi k}{\lambda^2} r^2. \tag{22}$$

Therefore, the energy density of the radio emission U_photon is

$$U_\mathrm{photon} \sim \frac{L_\nu \nu}{4\pi r^2 c} = \frac{2kT_\mathrm{e}\nu}{\lambda^2 c}. \tag{23}$$

Synchro-Compton Radiation

L_ν is the luminosity per unit bandwidth, and so the bolometric luminosity is roughly νL_ν. Therefore,

$$\eta = \frac{\left(\frac{2kT_\mathrm{e}\nu}{\lambda^2 c}\right)}{\left(\frac{B^2}{2\mu_0}\right)} = \frac{4kT_\mathrm{e}\nu\mu_0}{\lambda^2 c B^2}. \tag{24}$$

We can now use the theory of self-absorbed radio sources to express the magnetic flux density B in terms of observables. Repeating the calculations carried out in Sect. 6.8,

$$\nu_\mathrm{g} = \nu/\gamma^2 \quad \text{and} \quad 3kT_\mathrm{b} = 3kT_\mathrm{e} = \gamma m_\mathrm{e} c^2, \tag{25}$$

where T_b is the brightness temperature of the source. Reorganising these relations, we find

$$B = \frac{2\pi m_\mathrm{e}}{e}\left(\frac{m_\mathrm{e}c^2}{3kT_\mathrm{e}}\right)^2 \nu. \tag{26}$$

The Synchro-Compton Catastrophe

Therefore, the ratio of the loss rates, η, is

$$\eta = \frac{(\mathrm{d}E/\mathrm{d}t)_{\mathrm{IC}}}{(\mathrm{d}E/\mathrm{d}t)_{\mathrm{sync}}} = \left(\frac{81 e^2 \mu_0 k^5}{\pi^2 m_{\mathrm{e}}^6 c^{11}}\right) \nu T_{\mathrm{e}}^5. \tag{27}$$

This is the key result. It can be seen that the ratio of the loss rates depends very strongly upon the brightness temperature of the radio source. Putting in the values of the constants, we find that the critical brightness temperature is

$$T_{\mathrm{b}} = T_{\mathrm{e}} = 10^{12}\, \nu_9^{-1/5}\ \mathrm{K}, \tag{28}$$

where ν_9 is the frequency at which the brightness temperature is measured in units of 10^9 K, that is, in GHz. Thus, according to this calculation, no compact radio source should have brightness temperature greater than $T_{\mathrm{B}} \approx 10^{12}$ K, if the emission is incoherent synchrotron radiation.

VLBI Observations of Compact Sources

The most compact sources, which have been studied by VLBI at centimetre wavelengths, have brightness temperatures which are less than the synchro-Compton limit, typically, the values found being $T_{\rm B} \approx 10^{11}$ K, which is reassuring. Notice that this is direct evidence that the radiation is the emission of relativistic electrons since the temperature of the emitting electrons must be at least 10^{11} K.

This is not, however, the whole story. If the time-scales of variability τ of the compact sources are used to estimate their physical sizes, $l \sim c\tau$, the source regions must be considerably smaller than those inferred from VLBI, and then values of $T_{\rm B}$ exceeding 10^{11} K are found. It is likely that relativistic beaming is the cause of this discrepancy, a topic which we take up in a moment.

Band and Grindley (1985)

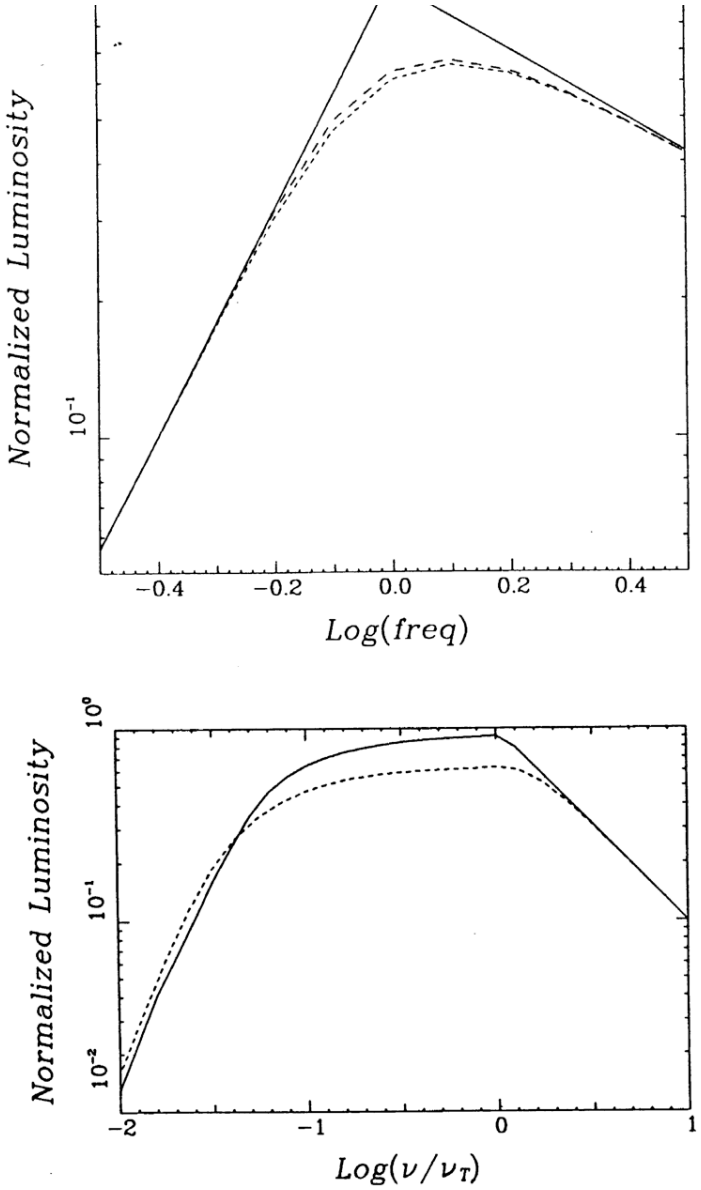

Examples of the expected spectra of sources of synchro-Compton radiation have been evaluated by Band and Grindlay (1985). They take into account the transfer of radiation within the self-absorbed source. The homogeneous source (top panel) has the standard form of spectrum, namely, a power-law distribution in the optically thin spectral region $L_\nu \propto \nu^{-\alpha}$, while, in the optically thick region, the spectrum has the form $L_\nu \propto \nu^{5/2}$. In the case of the inhomogeneous source (lower panel), the magnetic field strength and number density of relativistic electrons decrease outwards as power-laws, resulting in a much broader 'synchrotron-peak'.

Band and Grindley (1985)

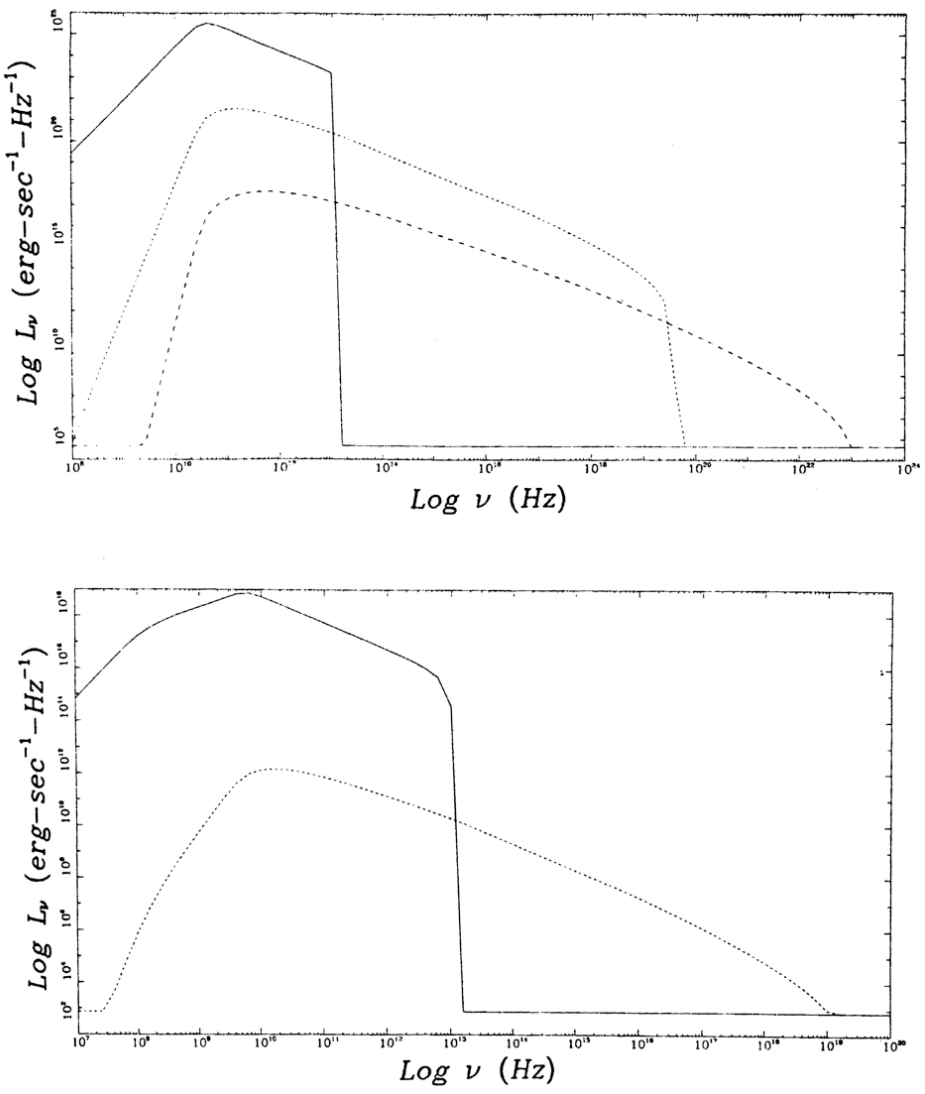

Of particular importance is that they take account of the fact that, at relativistic energies $h\nu \geq 0.5$ MeV, the Klein-Nishina cross-section rather than the Thomson cross-section should be used for photon-electron scattering. In the ultrarelativistic limit, the cross-section is

$$\sigma_{\rm KN} = \frac{\pi^2 r_{\rm e}^2}{h\nu}(\ln 2h\nu + \tfrac{1}{2}), \qquad (29)$$

and so the cross-section decreases as $(h\nu)^{-1}$ at high energies. Consequently, higher order scatterings result in much reduced luminosities as compared with the non-relativistic calculation.

Ultra-High Energy γ-ray Sources

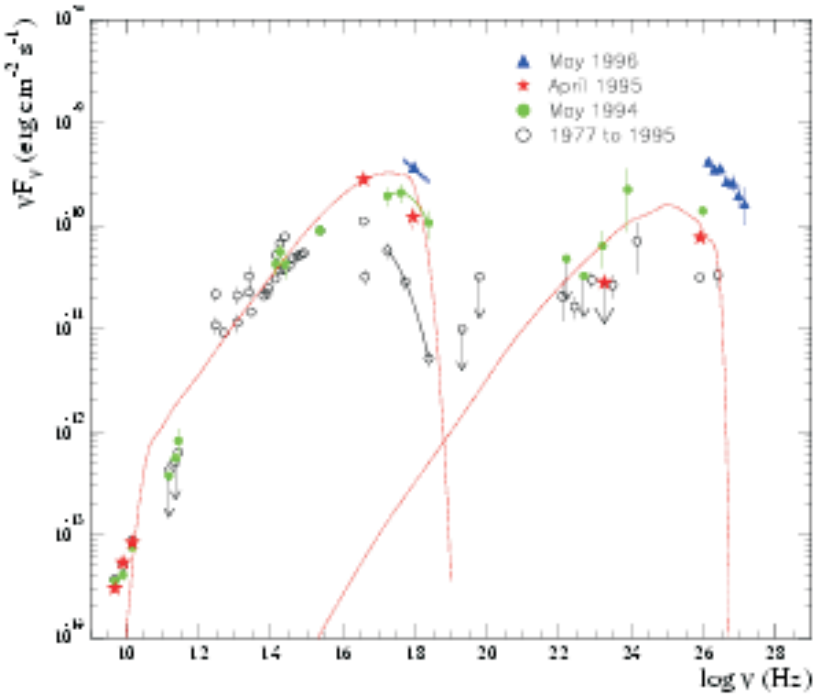

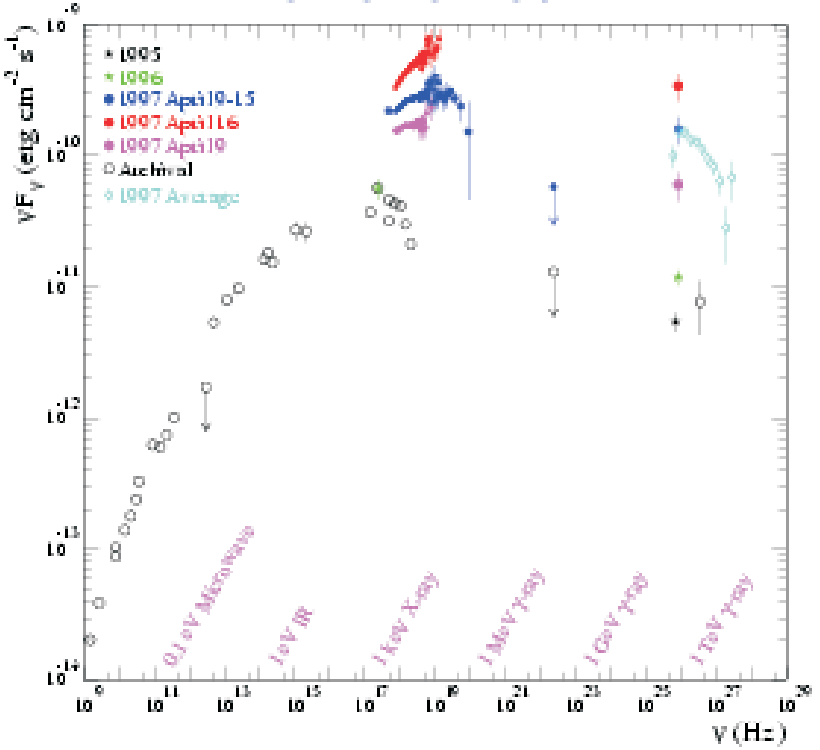

In the extreme γ-ray sources Markarian 421 and 501, it is very likely that some form of inverse Compton radiation is occurring, quite possible via the Synchro-Compton mechanism. These γ-ray sources are quite enormously luminous and variable. It is therefore likely that relativistic motions have to be involved to explain their luminosities and variability.

γ-ray Processes and Photon-Photon Interactions

The processes of synchrotron radiation, inverse Compton scattering and relativistic bremsstrahlung are effective means of creating high-energy γ-ray photons, but there are other mechanisms. One of the most important is the decay of neutral pions created in collisions between relativistic protons and nuclei of atoms and ions of the interstellar gas.

$$\mathrm{p} + \mathrm{p} \rightarrow \pi^{+}, \pi^{-}, \pi^{0}. \tag{30}$$

The charged pions decay into muons and neutrinos

$$\pi^{+} \rightarrow \mu^{+} + \nu_{\mu} \quad ; \quad \pi^{-} \rightarrow \mu^{-} + \bar{\nu}_{\mu} \tag{31}$$

with a mean lifetime of 2.551×10^{-8} s. The charged muons then decay with mean lifetime of 2.2001×10^{-6} s

$$\mu^{+} \rightarrow \mathrm{e}^{+} + \nu_{\mathrm{e}} + \bar{\nu}_{\mu} \quad ; \quad \mu^{-} \rightarrow \mathrm{e}^{-} + \bar{\nu}_{\mathrm{e}} + \nu_{\mu}. \tag{32}$$

Neutral Pions

In contrast, the neutral pions decay into pairs of γ-rays, $\pi^0 \rightarrow \gamma + \gamma$, in only 1.78×10^{-16} s. The cross-section for this process is $\sigma_{\mathrm{pp}\rightarrow\gamma\gamma} \approx 10^{-30}$ m^2 and the emitted spectrum of γ-rays has a broad maximum centred on a γ-ray energy of about 70 MeV (see *HEA2*, Sect. 20.1). This is the process responsible for the continuum emission of the interstellar gas at energies $\varepsilon \geq 100$ MeV. A simple calculation shows that, if the mean number density of the interstellar gas is $N \sim 10^6$ m^{-3} and the average energy density of cosmic ray protons with energies greater than 1 GeV about 10^6 eV m^{-3}, the γ-ray luminosity of the disc of our Galaxy is about 10^{32} W, as observed.

Electron-Positron Annihilation

Electron-positron annihilation can proceed in two ways. In the first case, the electrons and positrons annihilate at rest or in flight through the interaction $e^+ + e^- \rightarrow 2\gamma$. When emitted at rest, the photons both have energy 0.511 MeV. When the particles annihilate 'in flight', meaning that they suffer a fast collision, there is a dispersion in the photon energies. It is a pleasant exercise in relativity to show that, if the positron is moving with velocity v with corresponding Lorentz factor γ, the centre of momentum frame of the collision has velocity $V = \gamma v(1 + \gamma)$ and that the energies of the pair of photons ejected in the direction of the line of flight of the positron and in the backward direction are

$$E = \frac{m_e c^2(1+\gamma)}{2}\left(1 \pm \frac{V}{c}\right). \tag{33}$$

From this result, it can be seen that the photon which moves off in the direction of the incoming positron carries away most of the energy of the positron and that there is a lower limit to the energy of the photon ejected in the opposite direction of $m_e c^2/2$.

Electron-Positron Annihilation

If the velocity of the positron is small, *positronium atoms*, that is, bound states consisting of an electron and a positron, can form by radiative recombination: 25% of the positronium atoms form in the singlet $^1S_0$ state and 75% of them in the triplet $^3S_1$ state. The modes of decay from these states are different. The singlet $^1S_0$ state has a lifetime of 1.25×10^{10} s and the atom decays into two γ-rays, each with energy 0.511 MeV. The majority triplet $^3S_1$ states have a mean lifetime of 1.5×10^{-7} s and three γ-rays are emitted, the maximum energy being 0.511 MeV in the centre of momentum frame. In this case, the decay of positronium results in a continuum spectrum to the low energy side of the 0.511 MeV line. If the positronium is formed from positrons and electrons with significant velocity dispersion, the line at 0.511 MeV is broadened, both because of the velocities of the particles and because of the low energy wing due to continuum three-photon emission. This is a useful diagnostic tool in understanding the origin of the 0.511 MeV line. If the annihilations take place in a neutral medium with particle density less than $10^{21}\mathrm{m}^{-3}$, positronium atoms are formed. On the other hand, if the positrons collide in a gas at temperature greater than about 10^6 K, the annihilation takes place directly without the formation of positronium.

Electron-Positron Annihilation

The cross-section for electron-positron annihilation in the extreme relativistic limit is

$$\sigma = \frac{\pi r_e^2}{\gamma}[\ln 2\gamma - 1]. \tag{34}$$

For thermal electrons and positrons, the cross-section becomes

$$\sigma \approx \frac{\pi r_e^2}{(v/c)}. \tag{35}$$

Positrons are created in the decay of positively charged pions, π^+, which are created in collisions between cosmic ray protons and nuclei and the interstellar gas, roughly equal numbers of positive, negative and neutral pions being created. Since the π^0s decay into γ-rays, the flux of interstellar positrons created by this process can be estimated from the γ-ray luminosity of the interstellar gas. A second process is the decay of long-lived radioactive isotopes created by nucleosynthesis in supernova explosions. For example, the β^+ decay of ^{26}Al has a mean lifetime of 1.1×10^6 years. ^{26}Al is formed in supernova explosions and then ejected into the interstellar gas where the decay results in a flux of interstellar positrons.

Photon-Photon collisions

A third process is the creation of electron-positron pairs through *photon-photon collisions*, a process of considerable importance in compact γ-ray sources. Let us work out the threshold energy for this process. If $\boldsymbol{P}_1$ and $\boldsymbol{P}_2$ are the momentum four-vectors of the photons before the collision

$$\boldsymbol{P}_1 = [\varepsilon_1/c^2, (\varepsilon_1/c)\boldsymbol{i}_1] \quad ; \quad \boldsymbol{P}_2 = [\varepsilon_2/c^2, (\varepsilon_2/c)\boldsymbol{i}_2], \tag{36}$$

then conservation of four-momentum requires

$$\boldsymbol{P}_1 + \boldsymbol{P}_2 = \boldsymbol{P}_3 + \boldsymbol{P}_4 \tag{37}$$

where $\boldsymbol{P}_3$ and $\boldsymbol{P}_4$ are the four-vectors of the created particles. To find the threshold for pair production, we require that the particles be created at rest and therefore

$$\boldsymbol{P}_3 = [0, m_\mathrm{e}] \quad ; \quad \boldsymbol{P}_4 = [0, m_\mathrm{e}]. \tag{38}$$

Squaring both sides of (37) and noting that $\boldsymbol{P}_1 \cdot \boldsymbol{P}_1 = \boldsymbol{P}_2 \cdot \boldsymbol{P}_2 = 0$ and that $\boldsymbol{P}_3 \cdot \boldsymbol{P}_3 = \boldsymbol{P}_4 \cdot \boldsymbol{P}_4 = \boldsymbol{P}_3 \cdot \boldsymbol{P}_4 = m_\mathrm{e}^2 c^2$,

Photon-Photon Collisions

$$\boldsymbol{P}_1\cdot\boldsymbol{P}_1+2\boldsymbol{P}_1\cdot\boldsymbol{P}_2+\boldsymbol{P}_2\cdot\boldsymbol{P}_2 = \boldsymbol{P}_3\cdot\boldsymbol{P}_3+2\boldsymbol{P}_3\cdot\boldsymbol{P}_4+\boldsymbol{P}_4\cdot\boldsymbol{P}_4, \quad (39)$$

$$2\left(\frac{\varepsilon_1\varepsilon_2}{c^2}-\frac{\varepsilon_1\varepsilon_2}{c^2}\cos\theta\right) = 4m_{\rm e}^2c^2, \quad (40)$$

$$\varepsilon_2 = \frac{2m_{\rm e}^2c^4}{\varepsilon_1(1-\cos\theta)}, \quad (41)$$

where θ is the angle between the incident directions of the photons. Thus, if electron-positron pairs are created, the threshold for the process occurs for head-on collisions, $\theta=\pi$ and hence,

$$\varepsilon_2 \geq \frac{m_{\rm e}^2c^4}{\varepsilon_1} = \frac{0.26\times10^{12}}{\varepsilon_1}\,{\rm eV}, \quad (42)$$

where ε_1 is measured in electron volts. This process thus provides not only a means for creating electron-positron pairs, but also results an *important source of opacity* for very-high-energy γ-rays.

Photon-Photon Opacity

The table shows some important examples of combinations of ε_1 and ε_2. Photons with energies greater than those in the last column are expected to suffer some degree of absorption when they traverse regions with high energy densities of photons with energies listed in the first column.

	ε_1(eV)	ε_1(eV)
Microwave Background Radiation	6×10^{-4}	4×10^{14}
Starlight	2	10^{11}
X-ray	10^3	3×10^8

The cross-section for this process for head-on colisions in the ultrarelativistic limit is

$$\sigma = \pi r_{\rm e}^2 \frac{m_{\rm e}^2 c^4}{\varepsilon_1 \varepsilon_2} \left[2 \ln \left(\frac{2\omega}{m_{\rm e} c^2} \right) - 1 \right] \tag{43}$$

where $\omega = (\varepsilon_1 \varepsilon_2)^{1/2}$ and $r_{\rm e}$ is the classical electron radius.

Photon-Photon Opacity

In the limit $\hbar\omega \approx m_{\rm e}c^2$, the cross-section is

$$\sigma = \pi r_{\rm e}^2 \left(1 - \frac{m_{\rm e}^2 c^4}{\omega^2}\right)^{1/2} \tag{44}$$

Thus, near threshold, the cross-section for the interaction $\gamma\gamma \rightarrow {\rm e}^+{\rm e}^-$ is

$$\sigma \sim \pi r_{\rm e}^2 \sim 0.2\sigma_{\rm T}. \tag{45}$$

These cross-sections enable the opacity of the interstellar and intergalactic medium to be evaluated as well as providing a mechanism by which large fluxes of positrons could be generated in the vicinity of active galactic nuclei. These results are very important for the ultra-high γ-ray emission detected by instruments such as the HESS array in Namibia.

The Compactness Parameter

These considerations are particularly important in the case of the extremely luminous and highly variable extragalactic γ-ray sources discovered by the Compton Gamma-Ray Observatory (CGRO). A key role is played by the *compactness parameter*, which arises in considerations of whether or not a γ-ray source is opaque for $\gamma\gamma$ collisions because of pair production. Let us carry out a simple calculation which indicates how the compactness parameter arises. We will carry out the calculation for the flux of γ-rays at threshold, $\varepsilon \sim m_{\rm e}c^2$, for simplicity. The mean free path of the γ-ray for $\gamma\gamma$ collisions is $\lambda = (N_\gamma \sigma)^{-1}$ where N_γ is the number density of photons with energies $\varepsilon = h\nu \sim m_{\rm e}c^2$. If the source has luminosity L_γ and radius r, the number density of photons within the source region is

$$N_\gamma = \frac{L_\gamma}{4\pi r^2 c\varepsilon} \tag{46}$$

The condition for the source to be opaque is $r \approx \lambda$, that is,

$$r \sim \frac{4\pi r^2 c m_{\rm e}c^2}{L_\nu \sigma}, \quad \text{that is,} \quad \frac{L_\nu \sigma}{4\pi m_{\rm e}c^3 r} \sim 1 \tag{47}$$

The Compactness Parameter

The compactness factor C is defined to be the quantity

$$C = \frac{L_\nu \sigma}{4\pi m_e c^3 r} \tag{48}$$

If the compactness parameter is very much greater than unity, the γ-rays are destroyed by electron-positron pair production, resulting in a huge flux of electrons and positrons within the source region. Consequently, the source would no longer be a hard γ-ray source. Some of the intense γ-ray sources observed by the CGRO have enormous luminosities, $L_\gamma \sim 10^{41}$ W and vary significantly in intensity over time-scales of the order of days. Inserting these values into (48), it is found that $C \gg 1$ and so there is a problem in understanding why these sources exist. Fortunately, all the ultraluminous γ-ray sources are associated with compact radio sources, which exhibit synchrotron self-absorption and superluminal motions. The inference is that the luminosities of the γ-ray sources and the time-scales of variation have been significantly changed by the relativistic motion of the source region.

Superluminal Motions

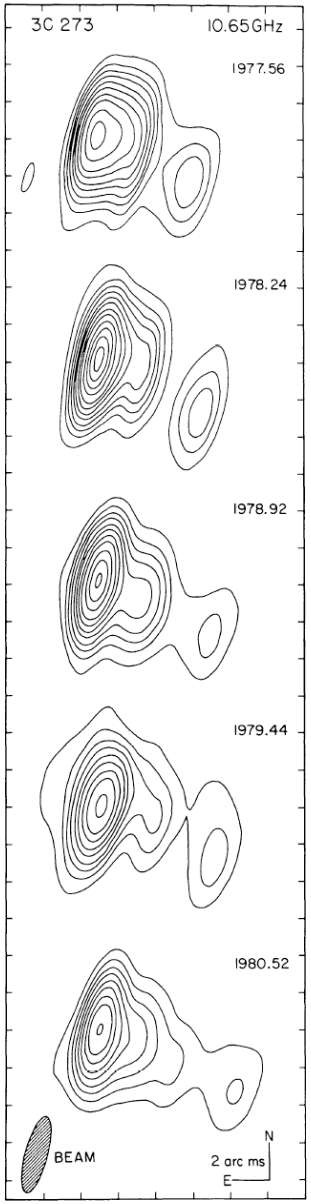

The most direct evidence comes from the superluminal motions observed in the compact radio jets found in VLBI observations of active galactic nuclei. In the classic case of the radio core of the radio source 3C 273, one of the radio components appeared to move a distance of 25 light-years in only three years, corresponding to an observed transverse velocity of about eight times the speed of light. This is a common phenomenon in the compact, variable radio sources which often have spectra which are synchrotron self-absorbed. The phenomenon has also been observed in Galactic radio sources, for example, the source GRS 1915+105, which is a binary X-ray source in which the compact X-ray source is associated with a stellar mass black hole (Mirabel and Rodriguez 1998).

Superluminal Motions

The observation of compact radio sources with brightness temperatures exceeding the critical value of 10^{12} K on the basis of their time variability is evidence that relativistic beaming may be required to overcome the Inverse Compton catastrophe.

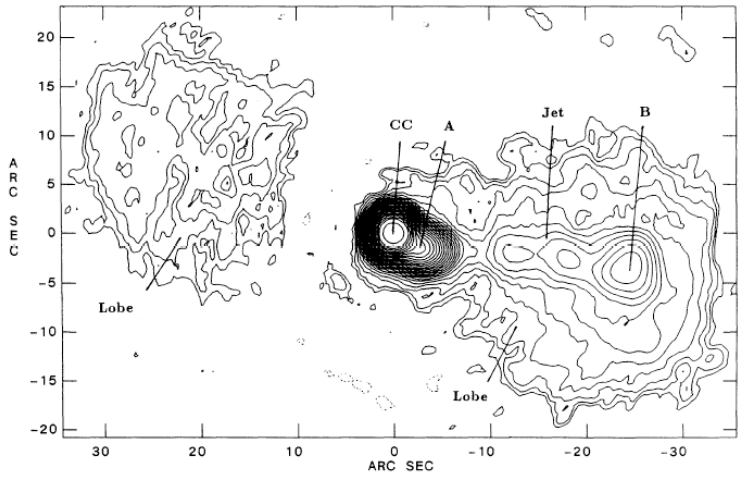

Relativistic beaming is the origin of the very rapid variations in intensity observed in some of the most extreme active galactic nuclei, the BL-Lac objects and blazars. If dimensions are estimated using the causality relation $l = c\tau$, where τ is the time-scale of the variability, the brightness temperature would exceed the critical value of 10^{12} K. A piece of evidence which supports this view of the BL-Lac phenomenon is the radio map of the blazar 3C 371. The central compact radio source is extended in the direction of a jet leading to one side of a classical double radio source.

Relativistic Ballistic Model

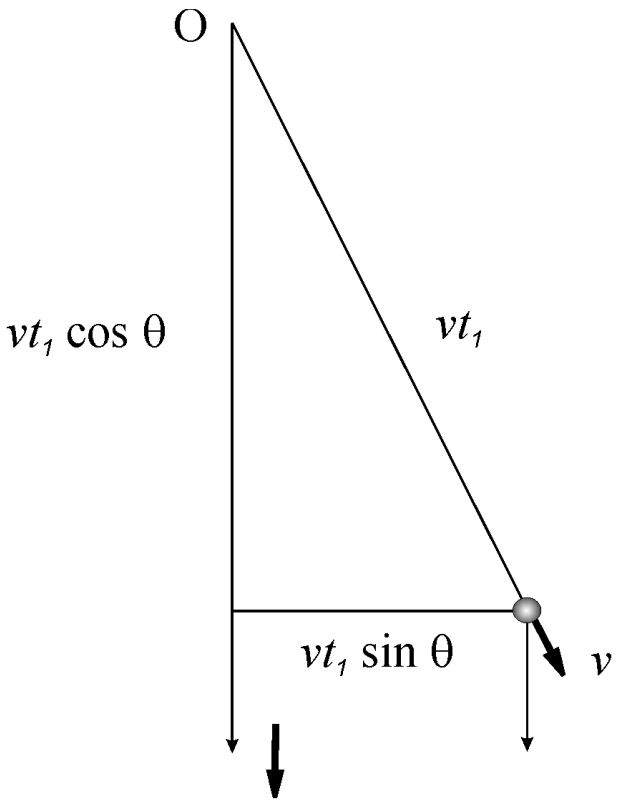

The motion of a relativistically moving source component as viewed from above.

Let us begin with the simplest, and most popular, model for superluminal sources, what is commonly referred to as the *relativistic ballistic model*. Let us carry out first the simplest part of the calculation, the determination of the *kinematics* of relativistically moving source components. The aim is to determine the observed transverse speed of a component ejected at some angle θ to the line of sight at a high velocity v.

The observer is located at a distance D from the source. The source component is ejected from the origin O at some time t_0 and the signal from that event sets off towards the observer, where it arrives at time $t = D/c$ later.

Relativistic Ballistic Model

After time t_1, the component is located at a distance vt_1 from the origin and so is observed at a projected distance $vt_1 \sin\theta$ according to the distant observer. The light signal bearing this information arrives at the observer at time

$$t_2 = t_1 + \frac{D - vt_1 \cos\theta}{c}, \tag{49}$$

since the signals have to travel a slightly shorter distance $D - vt_1 \cos\theta$ to reach the observer. Therefore, according to the distant observer, the transverse speed of the component is

$$v_\perp = \frac{vt_1 \sin\theta}{t_2 - t} = \frac{vt_1 \sin\theta}{t_1 - \dfrac{vt_1 \cos\theta}{c}} = \frac{v \sin\theta}{1 - \dfrac{v \cos\theta}{c}}. \tag{50}$$

It is a simple sum to show that the maximum observed transverse speed occurs at an angle $\cos\theta = v/c$ and is $v_\perp = \gamma v$, where $\gamma = (1 - v^2/c^2)^{-1/2}$ is the Lorentz factor.

Relativistic Ballistic Model

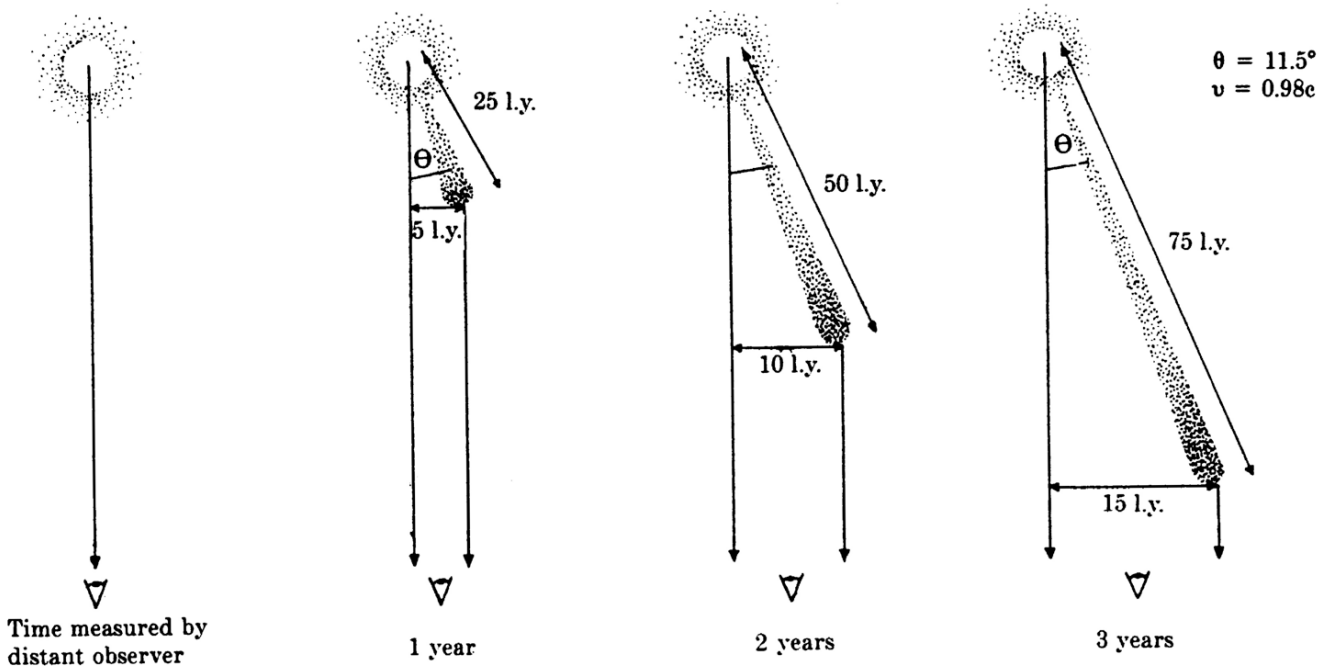

Thus, provided the source component moves at a speed close enough to the speed of light, apparent motions on the sky $v_\perp > c$ can be observed without violating causality and the postulates of special relativity. For example, if the the source component were ejected at a speed $0.98c$, transverse velocities up to $\gamma c = 5c$ are perfectly feasible, the case illustrated in the diagram.

Relativistic Aberration and Time Dilation

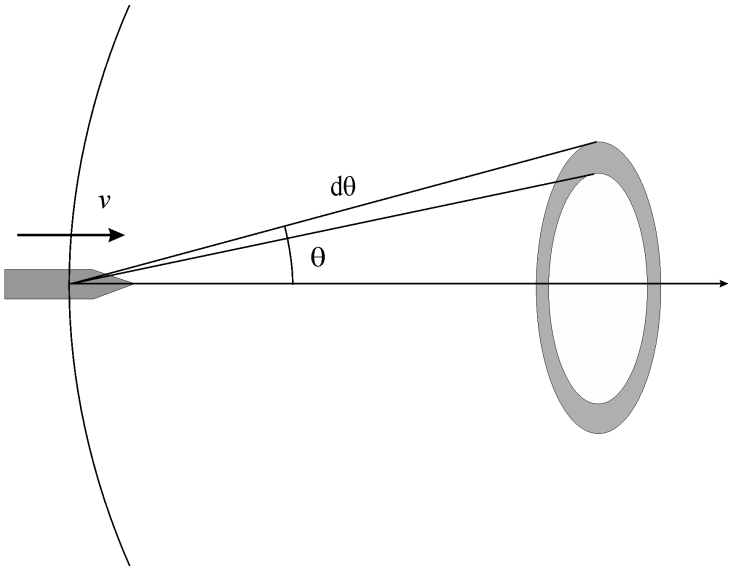

Let us consider first a classical undergraduate problem in relativity:

- *A rocket travels towards the Sun at speed* $v = 0.8c$*. Work out the luminosity, colour, angular size and brightness of the Sun as observed from the spaceship when it crosses the orbit of the Earth. It may be assumed that the Sun radiates like a uniform disc with a black-body spectrum at temperature* T_0*.*

This problem includes many of the effects found in relativistic beaming problems.

Relativistic Aberration and Time Dilation

Let us work out the separate effects involved in evaluating the intensity of radiation observed in the moving frame of reference.

- *The frequency shift of the radiation* The frequency four-vector in the frame of the Solar System S in Rindler's notation* is

$$\boldsymbol{K} = \left[\frac{\omega_0}{c}, -k_0\cos\theta, -k_0\sin\theta, 0\right], \tag{51}$$

  where the light rays are assumed to propagate towards the observer at the orbit of the Earth, as illustrated in the diagram. The frequency four-vector in the frame of reference of the spaceship S′ is

$$\boldsymbol{K}' = \left[\frac{\omega_0'}{c}, -k_0'\cos\theta', -k_0'\sin\theta', 0\right]. \tag{52}$$

*In Rindler's notation, the components of the four-vectors transform exactly as $[ct, x, y, z]$ according to the standard Lorentz transformation $ct' = \gamma(ct - Vx/c), x' = \gamma(x - Vt), y' = y, z' = z$. The invariant norm of the four-vector is $|R|^2 = c^2t^2 - x^2 - y^2 - z^2$.

Relativistic Aberration and Time Dilation

We use the time transform to relate the 'time'-components of the four-vectors:

$$ct' = \gamma\left(ct - \frac{Vx}{c}\right), \tag{53}$$

and so

$$\frac{\omega'}{c} = \gamma\left(\frac{\omega_0}{c} + \frac{Vk_0\cos\theta}{c}\right). \tag{54}$$

Since $k_0 = \omega_0/c$,

$$\nu' = \gamma\nu_0\left(1 + \frac{V}{c}\cos\theta\right) = \kappa\nu_0. \tag{55}$$

This is the expression for the 'blue-shift' of the frequency of the radiation due to the motion of the spacecraft.

- The *waveband* $\Delta\nu$, in which the radiation is observed, is blue shifted by the same factor

$$\Delta\nu' = \kappa\Delta\nu_0. \tag{56}$$

Relativistic Aberration and Time Dilation

- *Time intervals* are also different in the stationary and moving frames. This can be appreciated by comparing the periods of the waves as observed in S and S′

$$\nu' = \frac{1}{T'} \quad ; \quad \nu_0 = \frac{1}{T_0}, \tag{57}$$

and so

$$\frac{T'}{T} = \frac{\nu_0}{\nu'}. \tag{58}$$

Since the periods T and T' can be considered to be the times measured on clocks, the radiation emitted in the time interval Δt is observed in the time interval $\Delta t'$ by the observer in S′ such that

$$\Delta t' = \Delta t/\kappa. \tag{59}$$

Relativistic Aberration and Time Dilation

- *Solid Angles* It is simplest to begin with the cosine transform, which is derived from the 'x' Lorentz transformation of the frequency four-vector:

$$\cos\theta' = \frac{\cos\theta + \dfrac{V}{c}}{1 + \dfrac{V}{c}\cos\theta}. \tag{60}$$

Differentiating with respect to θ and θ' on both sides of this relation,

$$\sin\theta'\,\mathrm{d}\theta' = \frac{\sin\theta\,\mathrm{d}\theta}{\gamma^2\left(1 + \dfrac{V}{c}\cos\theta\right)^2} = \frac{\sin\theta\,\mathrm{d}\theta}{\kappa^2}. \tag{61}$$

This result has been derived for an annular solid angle with respect to the x-axis, but we can readily generalise to any solid angle since $\mathrm{d}\phi' = \mathrm{d}\phi$ and so

$$\sin\theta'\,\mathrm{d}\theta'\,\mathrm{d}\phi' = \frac{\sin\theta\,\mathrm{d}\theta\,\mathrm{d}\phi}{\kappa^2} \qquad \mathrm{d}\Omega' = \frac{\mathrm{d}\Omega}{\kappa^2}. \tag{62}$$

The solid angle in S$'$ is smaller by a factor κ^2 as compared with that observed in S. This is a key aspect of the derivation of the aberration formulae.

Relativistic Aberration and Time Dilation

We can now put these results together to work out how the intensity of radiation from the region of the Sun within solid angle $\mathrm{d}\Omega$ changes between the two frames of reference. The intensity $I(\nu)$ is the power arriving at the observer per unit frequency interval per unit solid angle from the direction θ. The observer in the spacecraft observes the radiation arriving in the solid angle $\mathrm{d}\Omega'$ about the angle θ' and so we transform its other properties into S$'$. The energy $h\nu N(\nu)$ received in S in the time interval Δt, in the frequency interval $\Delta\nu$ and in solid angle $\Delta\Omega$ is observed in S$'$ as an energy $h\nu' N(\nu')$ in the time interval $\Delta t'$, in the frequency interval $\Delta\nu'$ and in solid angle $\Delta\Omega'$, where $N(\nu) = N(\nu')$ is the invariant number of photons. Therefore, the intensity observed in S$'$ is

$$I(\nu') = I(\nu) \times \frac{\kappa \times \kappa \times \kappa^2}{\kappa} = I(\nu)\kappa^3. \tag{63}$$

Now, let us apply this result to the spectrum of black-body radiation, for which

$$I(\nu) = \frac{2h\nu^3}{c^2}\left(\mathrm{e}^{h\nu/kT} - 1\right)^{-1}. \tag{64}$$

Relativistic Aberration and Time Dilation

Then,

$$I(\nu') = \frac{2h\nu^3\kappa^3}{c^2}\left(\mathrm{e}^{h\nu/kT} - 1\right)^{-1} = \frac{2h\nu'^3}{c^2}\left(\mathrm{e}^{h\nu'/kT'} - 1\right)^{-1}, \qquad (65)$$

where $T' = \kappa T$. In other words, the observer in S′ observes a black-body radiation spectrum with temperature $T' = \kappa T$. A number of useful results follow from this analysis. For example, (65) describes the temperature distribution of the Cosmic Microwave Background Radiation over the sky as observed from the Solar System which is moving through the frame of reference in which the sky would be perfectly isotropic on the large scale at a velocity of about 600 km s^{-1}. Since $V/c \approx 2 \times 10^{-3}$ and $\gamma \approx 1$, the temperature distribution is rather precisely a dipole distribution, $T = T_0[1 + (V/c)\cos\theta]$ with respect to the direction of motion of the Solar System through the Cosmic Microwave Background Radiation.

In the example of the spacecraft travelling at $v = 0.8c$ towards the Sun, we can illustrate a number of the features of relativistic beaming. In this case, $\gamma = 5/3$ and the angle at which there is no change of temperature, corresponding to $\gamma[1 + (V/c)\cos\theta] = 1$, is $\theta = 60°$.

Relativistically Moving Source Components

Let us now turn to the case of relativistically moving source components. We need to determine the value of κ for the source component moving at velocity V at an angle θ with respect to the line of sight from the observer to the distant quasar. In this case, a straightforward calculation shows that the value of κ is

$$\kappa = \frac{1}{\gamma\left(1 - \frac{V\cos\theta}{c}\right)}, \tag{66}$$

where the source is moving towards the observer as illustrated in the figure. Just as in the above example, the observed flux density of the source is therefore

$$S(\nu_{\rm obs}) = \frac{L(\nu_0)}{4\pi D^2} \times \kappa^3, \tag{67}$$

where $\nu_{\rm obs} = \kappa\nu_0$. In the case of superluminal sources, the spectra can often be described by a power-law $L(\nu_0) \propto \nu_0^{-\alpha}$ and so

$$S(\nu_0) = \frac{L(\nu_0)}{4\pi D^2} \times \kappa^{3+\alpha}. \tag{68}$$

Relativistically Moving Source Components

Thus, if the superluminal sources consisted of identical components ejected from the radio source at the same angle to the line of sight in opposite directions, the relative intensities of the two components would be in the ratio

$$\frac{S_1}{S_2} = \left(\frac{1 + \frac{v}{c}\cos\theta}{1 - \frac{v}{c}\cos\theta} \right)^{3+\alpha} . \tag{69}$$

It is therefore expected that there should be large differences in the observed intensities of the jets. For example, if we adopt the largest observed velocities for a given value of γ, $\cos\theta = v/c$, then in the limit $v \approx c$,

$$\frac{S_1}{S_2} = \left(2\gamma^2\right)^{3+\alpha} . \tag{70}$$

Thus, since values of $\gamma \sim 10$ are quite plausible and $\alpha \sim 0 - 1$, it follows that the advancing component would be very much more luminous than the receding component. It is, therefore, not at all unexpected that the sources should be one-sided.

Relativistically Moving Source Components

Another complication is the fact that the emission is often assumed to be associated with jets. If the jet as a whole is moving at velocity v, then the time dilation formula shows that the advancing component is observed in a different proper time interval as compared with the receding component, the time which has passed in the frame of the source being $\Delta t_1 = \kappa \Delta t_0$ where Δt_0 is the time measured in the observer's frame of reference. If the jet consisted of a stream of components ejected at a constant rate from the active galactic nucleus, the observed intensity of the jet would be enhanced by a factor of only $\kappa^{2+\alpha}$. Thus, the precise form of the relativistic beaming factor is model dependent and care needs to be taken about the assumptions made.

Let us consider the case of sources exceeding the limiting surface brightness $T_{\rm b} = 10^{12}$ K. In the case of the *Inverse Compton Catastrophe*, the ratio of the loss rates for inverse Compton scattering and synchrotron radiation depends upon the product $\nu T_{\rm b}^5$. Since the brightness temperature $T_{\rm obs} = \kappa^5 T_0$ and $\nu_{\rm obs} = \kappa \nu_0$, it follows that $\eta \propto \kappa^6$. Thus, the observed value of $T_{\rm b}$ can exceed 10^{12} K if $\kappa \gg 1$.

Relativistically Moving Source Components

In the case of the *compactness parameter*,

$$C = \frac{L_\nu \sigma_{\mathsf{T}}}{4\pi m_{\mathsf{e}} c^3 \times ct}, \tag{71}$$

the relativistic beaming factors enable us to understand why these sources should exist. In the simple argument in which the source components are at rest, it is assumed that the dimensions of the source are $l \approx ct$ from its rapid time variability. The observed luminosity is enhanced by a factor $\kappa^{3+\alpha}$ and, in addition, because the time-scale of variability appears on the denominator, the observed value is shorter by a factor κ and so the compactness parameter is increased by relativistic beaming by a factor of roughly $\kappa^{4+\alpha}$. Since $\alpha \approx 1$, it can be seen that $C \propto \kappa^5$ and so, in the frame of the source components themselves, the value of the compactness parameter can be reduced below the critical value.

The Acceleration of Charged Particles

This is a huge subject of importance for many aspects of high energy astrophysics and there is only space to give a brief impression of the mechanism which now dominates much of the thinking in the field. The preferred mechanism is involves *first order Fermi acceleration of particles in strong shock waves*. Let us begin with a simple general formulation of the acceleration process in which the average energy of the particle after one collision is $E = \beta E_0$ and the probability that the particle remains within the accelerating region after one collision is P. Then, after k collisions, there are $N = N_0 P^k$ particles with energies $E = E_0 \beta^k$. Eliminating k between these quantities,

$$\frac{\ln(N/N_0)}{\ln(E/E_0)} = \frac{\ln P}{\ln \beta}, \tag{72}$$

and hence

$$\frac{N}{N_0} = \left(\frac{E}{E_0}\right)^{\ln P/\ln \beta}. \tag{73}$$

Fermi Acceleration

In fact, this value of N is $N(\geq E)$, since this number reach energy E and some fraction of them is accelerated to higher energies. Therefore,

$$N(E)\,\mathrm{d}E = \text{constant} \times E^{-1+\ln P/\ln \beta}\,\mathrm{d}E. \tag{74}$$

Notice that we have obtained a power-law energy spectrum of the particles, exactly what is required to account for the non-thermal spectra of many different classes of high energy astrophysical sources.

In Fermi's original version of the *Fermi mechanism*, α was proportional to $(V/c)^2$, because of the decelerating effect of the following collisions. The original version of Fermi's theory is therefore known as *second order Fermi acceleration* and is a very slow process. We would do much better if there were only head-on collisions, in which case the energy increase would be $\Delta E/E \propto V/c$, that is, first-order in V/c and, appropriately, this is called *first-order Fermi acceleration*.

First-order Fermi Acceleration

A very attractive version of first-order Fermi acceleration in the presence of strong shock waves was discovered independently by a number of workers in the late 1970s. The papers by Axford, Leer and Skadron (1977), Krymsky (1977), Bell (1978) and Blandford and Ostriker (1978) stimulated an enormous amount of interest in this process for the many environments in which high energy particles are found in astrophysics. There are two different ways of tackling the problem. One starts from the diffusion equation for the evolution of the momentum distribution of high energy particles in the vicinity of strong shock waves (for example, Blandford and Ostriker 1978).

The second is a more physical approach in which the behaviour of individual particles is followed (for example, Bell 1978). Let us adopt Bell's version of the theory which makes the essential physics clear and indicates why this version of first order Fermi acceleration results remarkably naturally in a power-law energy spectrum of high energy particles.

First-order Fermi Acceleration

To illustrate the basic physics of the acceleration process, let us consider the case of a strong shock propagating through the interstellar medium. A flux of high energy particles is assumed to be present both in front of and behind the shock front. The particles are considered to be of very high energy and so the velocity of the shock is very much less than those of the high energy particles.

The key point about the acceleration mechanism is that the high energy particles hardly notice the shock at all since its thickness is normally very much smaller than the gyroradius of a high energy particle. Because of turbulence behind the shock front and irregularities ahead of it, when the particles pass though the shock in either direction, they are scattered so that their velocity distribution rapidly becomes isotropic on either side of the shock front. The key point is that the distributions are isotropic with respect to the frames of reference in which the fluid is at rest on either side of the shock.

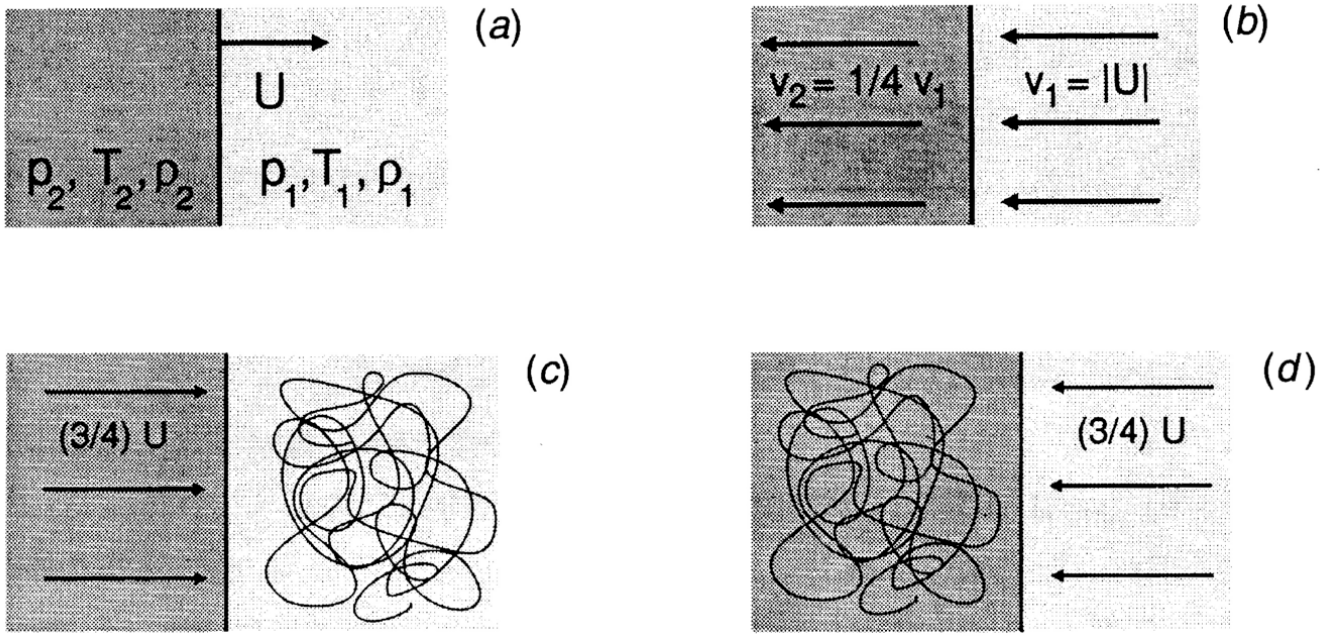

It is often convenient to transform into the frame of reference in which the shock front is at rest and then the up-stream gas flows into the shock front at velocity $v_1 = U$ and leaves the shock with a downstream velocity v_2. The equation of continuity requires mass to be conserved through the shock and so

$$\rho_1 v_1 = \rho_2 v_2.$$

In the case of a strong shock, $\rho_2/\rho_1 = (\gamma + 1)/(\gamma - 1)$ where γ is the ratio of specific heats of the gas. Taking $\gamma = 5/3$ for a monatomic or fully ionised gas, we find $\rho_2/\rho_1 = 4$ and so $v_2 = (1/4)v_1$ (see figure (b)).

Now let us consider the high energy particles ahead of the shock. Scattering ensures that the particle distribution is isotropic in the frame of reference in which the gas is at rest. It is instructive to draw diagrams illustrating the dynamical situation so far as typical high energy particles upstream and downstream of the shock are concerned. Let us consider the upstream particles first. The shock advances through the medium at velocity U but the gas behind the shock travels at a velocity $(3/4)U$ relative to the upstream gas (c). When a high energy particle crosses the shock front, it obtains a small increase in energy, of the order $\Delta E/E \sim U/c$. The particles are then scattered by the turbulence behind the shock front so that their velocity distributions become isotropic with respect to that flow.

Now let us consider the opposite process of the particle diffusing from behind the shock to the upstream region in front of the shock (Figure d). Now the velocity distribution of the particles is isotropic behind the shock and, when they cross the shock front, they encounter gas moving towards the shock front again with the same velocity $(3/4)U$. In other words, the particle undergoes exactly the same process of receiving a small increase in energy ΔE on crossing the shock from downstream to upstream as it did in travelling from upstream to downstream.

This is the clever aspect of this acceleration mechanism. Every time the particle crosses the shock front it receives an increase of energy, there are never crossings in which the particles lose energy, and the increment in energy is the same going in both directions. Thus, unlike the standard Fermi mechanism in which there are both head-on and following collisions, in the case of strong shock fronts, the collisions are always head-on and energy is transferred to the particles. The beauty of the mechanism is the complete symmetry between the passage of the particles from upstream to downstream and from downstream to upstream through the shock wave.

Results of Simple Calculations

The average energy gain when particles cross from one side of the shock to the other is

$$\left\langle \frac{\Delta E}{E} \right\rangle = \tfrac{2}{3}\frac{V}{c}, \tag{75}$$

the factor of $\frac{2}{3}$ coming from averaging over all angles of incidence of the particles with respect to the shock wave. $V = \frac{3}{4}U$ is the speed of the material behind the shock. Thus, in one round trip, the fractional energy gain is

$$\left\langle \frac{\Delta E}{E} \right\rangle = \tfrac{4}{3}\frac{V}{c} = \frac{U}{c}, \tag{76}$$

The other factor we need is the fraction of the particles which are lost per cycle. Particles are lost by being 'advected' downstream by the flow of gas behind the shock, the downstream flux being $\frac{1}{4}UN$, whereas the number of particles crossing the shock is $\frac{1}{4}Nc$. Thus, the loss probability is the ratio of these fluxes U/c and the probability of the particles remaining within the accelerating region is

$$P = 1 - \frac{U}{c}. \tag{77}$$

Therefore,

$$\ln\beta = \ln\left(1 + \frac{4V}{3c}\right) = \frac{4V}{3c} = \frac{U}{c} \qquad \ln P = \ln\left(1 - \frac{U}{c}\right) = -\frac{U}{c}. \tag{78}$$

Inserting these values into (3), we find

$$\ln P/\ln\beta = -1, \tag{79}$$

and so the differential spectrum of the accelerated electrons is

$$N(E)\,\mathrm{d}E \propto E^{-1+\ln P/\ln\beta}\,\mathrm{d}E = E^{-2}\,\mathrm{d}E. \tag{80}$$

This is the remarkable result of this version of first-order Fermi acceleration. The predicted spectrum is of power-law form with spectral index -2, corresponding to a synchrotron emission spectrum $\alpha = 0.5$. It may be argued that this is a somewhat flatter spectrum than that of many non-thermal galactic and extragalactic sources. Nonetheless, it is a remarkable result that roughly the correct form of spectrum is found, particularly when it is appreciated that the result depends only upon the assumption that the particles diffuse back and forth across a strong shock wave.